

Holographic dual of QCD from black D5 branes

This article has been downloaded from IOPscience. Please scroll down to see the full text article.

JHEP08(2009)057

(<http://iopscience.iop.org/1126-6708/2009/08/057>)

[The Table of Contents](#) and [more related content](#) is available

Download details:

IP Address: 80.92.225.132

The article was downloaded on 03/04/2010 at 10:21

Please note that [terms and conditions apply](#).

Holographic dual of QCD from black D5 branes

Benjamin A. Burrington^a and Jacob Sonnenschein^b

^a*Department of Physics, University of Toronto,
Toronto, Ontario, M5S 1A7 Canada*

^b*School of Physics and Astronomy, The Raymond and Beverly Sackler Faculty of Exact Sciences,
Tel Aviv University, Ramat Aviv, 69978, Israel*

E-mail: bburrin@umich.edu, cobi@post.tau.ac.il

ABSTRACT: We study the dynamics of probe D7 $\overline{D7}$ flavor probe branes in the background of near extremal D5 branes. This model is a holographic dual to a gauge theory with spontaneous breaking of a $U(N_f)_L \times U(N_f)_R$ chiral symmetry. The spectrum of two such D7 $\overline{D7}$ embeddings, contains a single massive 4D meson coming from the world volume $U(1)$ gauge field, the pion, and a single massive 4D scalar meson coming from fluctuations of the embedding of the brane. In addition, there are continuum five dimensional states due to the finite height of the effective potential in the radial direction. We investigate baryons in this model, and find that the size is stabilized due to the Chern-Simons term in the D7 world volume action. The model admits a Hagedorn temperature of $\frac{1}{2\pi R}$ where R is the radius parameter in the D5 branes metric. We investigate the pattern of chiral symmetry breaking in the deconfined phase as a function of the asymptotic separation of the branes L . We find that for $\frac{\pi}{3}R < L \lesssim 1.068R$ that chiral symmetry is restored, and that chiral symmetry is broken for L outside this window. We further argue that the solutions with $L < \frac{\pi}{3}$ are only classically stable, and in fact no D7 embedding exists with these boundary conditions.

KEYWORDS: Gauge-gravity correspondence, Intersecting branes models, AdS-CFT Correspondence

ARXIV EPRINT: [0903.0628](https://arxiv.org/abs/0903.0628)

Contents

1	Introduction	1
2	D7 embeddings	4
2.1	Mesons in the model	9
2.1.1	Vector mesons	11
3	Large $u_0 \gg u_\Lambda$ limit	12
3.1	Scalar mesons	16
3.2	Vector mesons	18
4	A simple antipodal embedding	19
4.1	Scalar mesons	19
4.2	Vector mesons	22
4.3	Baryons	23
5	Deconfined phase	26
6	Conclusions, and outlook	29

1 Introduction

QCD at strong coupling has several properties of interest: Confinement, the existence and spectrum of bound states, and chiral symmetry breaking to name a few. Studying these phenomena from the standpoint of quantum field theory is difficult, and impossible when confined to the realm of perturbation theory.

Recently, much progress has been made by constructing brane background models with a tunable parameter, such that in one limit they become pure (weakly coupled) $SU(N_c)$ QCD, and in the opposite they become a weakly coupled string theory [1]. Such constructions allow one to study a model that is in the same universality class as pure YM theory via gauge gravity duality [2] (for a review see [3]). Karch and Katz [4] introduced a holographic dual of dynamical flavored fundamental quarks by adding flavor probe D-branes into the gravity background. By taking the number of flavor branes to be much smaller than N_c , $N_f \ll N_c$, the backreaction on the background is avoided. This is the analog of the quenched approximation in the gauge theory. This was done originally for non-confining backgrounds. In [5] a similar scenario was proposed in a confining setup.¹ The incorporation of chiral symmetry and its spontaneous breakdown has been done in the

¹For references of additional papers that discussed holographic dynamical quarks see [6].

seminal papers of Sakai and Sugimoto (SS)[7, 8]. Their model which has been extensively studied in the literature.

In the SS model, the background is taken to be a near extremal D4 with one of the spatial coordinates compactified, which we will call x_4 , and its radius of compactification is R_{x_4} . For energies $E \ll \frac{1}{R_{x_4}}$ one expects 4D dynamics contaminated with KK modes. In the low temperature regime, the correct place to put the blackening factor is in front of the dx_4^2 component of the metric, giving the u, x_4 plane the geometry of a (semi-infinite) “cigar”. The probe flavor branes are taken to be (N_f) D8 branes, and are parallel to some combination of the radial direction, parameterized by u , and x_4 . In this model, the realization of chiral symmetry breaking $U(N_f)_R \times U(N_f)_L \rightarrow U(N_f)$ is geometric, and easy to visualize: the stack of D8 branes must connect smoothly at the bottom of the cigar, and so connect smoothly out to $\overline{D8}$ branes at infinity, making a U-shaped profile in the u, x_4 plane. At large u , the UV, one sees a disconnected $D8 \overline{D8}$ pair with $U(N_f)_R \times U(N_f)_L$ which is broken at small u , the IR, where one sees only the diagonal $U(N_f)$ symmetry remaining. A variety of physical properties of meson and baryon physics has been extracted from the model. These include the massive meson spectrum, the massless Goldstone pions [7], certain decay rates [8], thermal behavior of hadrons [9, 10], as well as describing certain condensation phenomena in the theory [11–17]. It is clear, however, that the SS model is far from being the ultimate gravity dual of QCD. It suffers from several drawbacks like the fact that its UV completion is not known, like discrepancies between its hadronic spectrum and that observed in nature. Thus, one is instructed to further construct holographic laboratories. The present paper follows these lines.

Here, we will instead take a near extremal D5 background with two of the world volume coordinates compactified (x_4, x_5) , and take the flavor branes to be probe D7 branes. We take probe D7 branes will be parallel to some combination of u, x_4, x_5 ; some aspects of this setup have been investigated in [18], and a close analog investigated in [19]. We expect that the low energy dynamics to be once again 4D, and given the arguments of [1] (and applied to the D5 background in [19]), should also be in the same universality class as pure YM theory, excluding the flavor branes. Including the flavor branes adds chiral fermions to the low energy weak coupling description, and so the holographic setup is dual to a theory in the same universality class as pure large N_c QCD.

There are, however, some key differences between extremal D4 and D5 branes. Most distinctly is the fact that the decoupling limit does not raise a large barrier, decoupling the bulk modes. Rather, the radial effective potential becomes infinitely long, but of finite height. We find that this is true for the effective potential of the D7 brane fluctuations as well. This gives that the effective potential has finitely many bound states, and so unfortunately only a finite number of 4D mesons. We will, however, see the same type of geometric understanding of chiral symmetry breaking as described above.

To begin, we will now briefly review the near horizon limit of the near extremal D5 background we wish to study. The metric is given by

$$ds^2 = \frac{u}{R} (\eta_{\mu\nu} dx^\mu dx^\nu + dx_4^2 + dx_5^2 f(u; u_\Lambda)) + \frac{R}{u} \frac{du^2}{f(u; u_\Lambda)} + Rud\Omega_3^2 \quad (1.1)$$

where $d\Omega_3^2$ is the metric of the unit 3 sphere, and

$$f(u; u_\Lambda) = \left(1 - \frac{u_\Lambda^2}{u^2}\right). \quad (1.2)$$

Furthermore, there is a non trivial dilaton and 3 form flux

$$\exp \phi = g_s \frac{u}{R}, \quad F_3 = \frac{2R^2}{g_s} \Omega_3 \quad (1.3)$$

where Ω_3 is the volume form of the unit 3 sphere. The parameter R is related to string parameters in the usual way $R^2 = g_s N_c \alpha'$. We will be considering the case where both x_4 and x_5 are compact

$$x_4 = x_4 + 2\pi R_{x_4}, \quad x_5 = x_5 + 2\pi R_{x_5}. \quad (1.4)$$

The parameter R_{x_5} is in fact not independent of the other scales already mentioned, given that we want the solution to be smooth around $u = u_\Lambda$. One can see this most easily by changing to variables

$$u^2 = u_\Lambda^2 + z^2. \quad (1.5)$$

In these variables, the metric reads

$$ds^2 = \frac{\sqrt{u_\Lambda^2 + z^2}}{R} (\eta_{\mu\nu} dx^\mu dx^\nu + dx_4^2) + R \sqrt{u_\Lambda^2 + z^2} d\Omega_3^2 + \frac{R \left(dz^2 + z^2 \frac{dx_5^2}{R^2} \right)}{\sqrt{u_\Lambda^2 + z^2}} \quad (1.6)$$

and clearly, for the metric to be non singular around $z = 0$, we need to take

$$x_5 = x_5 + 2\pi R, \quad \text{i.e. } R_{x_5} = R. \quad (1.7)$$

Thus we see that unlike the SS here u_Λ is a free parameter not related to R . In fact this is the situation classically. Based on similar situations [20], it is plausible that quantum mechanically the system will not be stable for any u_Λ . However, for the case discussed in section 3 this instability does not occur. One should also note that the above background is confining, as $\sqrt{g_{tt}g_{xx}}$ is finite.

For this background, we read off the relation between field theory and string theory quantities

$$g_6^2 = (2\pi)^3 g_s \alpha', \quad g_4^2 = \frac{2\pi g_s \alpha'}{R R_{x_4}} \\ T_{st} = \frac{1}{2\pi \alpha'} \sqrt{g_{tt}g_{xx}}|_{u=u_\Lambda} = \frac{u_\Lambda}{2\pi \alpha' R}. \quad (1.8)$$

The fact that u_Λ is a free parameter implies that so is the string tension. Further, we should comment that this background is S-dual to the near extremal NS5 brane. Such NS5 brane constructions have been argued to be the holographic dual of little string theories (LSTs) [21] (for a review, see [22]), however in the case at hand we are in the opposite range of validity ($g_s \ll 1$). Further, because S duality works non trivially on the D7 brane probes, our theory will not have a straightforward UV completion. The use of holographic

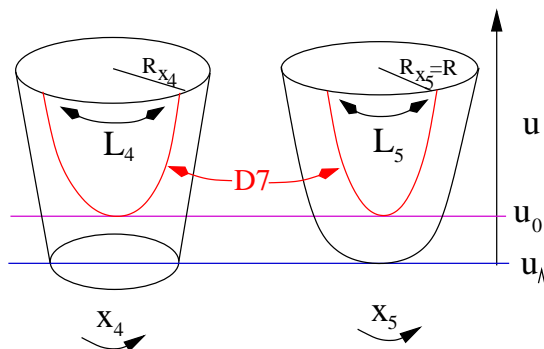


Figure 1. The configuration of D7 branes in the near extremal D5 brane background, following the above considerations.

techniques for the NS backgrounds, [23–25], should, however, be easily be adapted to our scenario (and in some cases be identical).

We organize the remainder of the paper as follows. In section 2 we discuss the general behavior for D7 embeddings in the confined phase, and briefly discuss the eigenvalue problem to describe the masses of mesons in this general case. In section 3, we consider D7 embeddings into the extremal limit of the background, which is also sufficient to describe D7 embeddings that do not come near to the end of the radial coordinate at $u = u_\Lambda$. We find that these embeddings obey a simple scaling behavior, which we describe generally enough to be applicable outside of these particular models. We also consider fluctuations of the embedding functions and the world volume gauge field to describe the spectrum of mesons in this limit. In section 4, we describe an embedding that falls all the way to $u = u_\Lambda$, and again consider fluctuations of the embedding functions and world volume gauge field. We also consider baryons in this scenario. Finally, in section 5 we consider the deconfined case, and consider the pattern of chiral symmetry breaking as a function of the boundary conditions. In section 6 we conclude, and suggest some future lines of investigation.

2 D7 embeddings

In this section we will consider embeddings of D7 branes into the above background. Qualitatively, we will find embedding of the form shown in figure 1. This background is similar to the paperclip or hairpin background (see for instance [26] and [27]). The embeddings we consider are transverse to some combination of the u, x_4, x_5 directions, and so the Chern Simons (CS) term will be unimportant in determining the solutions of the equations of motion, and we are left with the Dirac-Born-Infeld (DBI) action

$$S_{D7} = -\kappa_7 \int d^8\xi \exp(-\phi) \sqrt{\left(-\det\left(g_{MN} \frac{\partial X^M}{\partial \xi^i} \frac{\partial X^N}{\partial \xi^j}\right)\right)} \quad (2.1)$$

where we have used the notation ξ^i to represent world volume coordinates of the D7 brane, and κ_7 is the D7 tension. We use an Ansatz of the form

$$\begin{aligned} x^i(\xi) &= \xi^i, & i = \mu, \quad i = \text{sphere coordinate} \\ x_5(\xi) &= x_5(\rho), \quad x_4(\xi) = x_5(\rho), \quad u(\xi) = u(\rho). \end{aligned} \quad (2.2)$$

In the above notation, we have picked a “static gauge” for the x^μ and sphere directions. The final world volume coordinate, ρ , parameterizes a path in x_4, x_5, u space. One can show directly that the full non linear equations of motion for the x^μ and sphere directions are satisfied for the above Ansatz. Using the reparameterization invariance in ρ , we make one final choice

$$u(\rho) = \rho. \quad (2.3)$$

We now reduce the action to 1 dimension (ρ) and find the relevant equations of motion. In the following we will abbreviate $\frac{\partial}{\partial \rho} = \partial$. Using this notation, the action becomes

$$S_{D7} = \frac{\kappa_7 V_3 V_4}{g_s} \int d\rho \rho^3 \sqrt{(\partial x_4)^2 + (\partial x_5)^2 f(\rho; u_\Lambda) + \frac{R^2}{\rho^2 f(\rho; u_\Lambda)}}. \quad (2.4)$$

The equations of motion are quite simple, and follow from the Noether charges associated with translation invariance in x_4 and x_5 . These read

$$\frac{\rho^3 \partial x_4}{\sqrt{(\partial x_4)^2 + (\partial x_5)^2 f(\rho; u_\Lambda) + \frac{R^2}{\rho^2 f(\rho; u_\Lambda)}}} = P_4 u_\Lambda^3 \quad (2.5)$$

$$\frac{\rho^3 f(\rho; u_\Lambda) \partial x_5}{\sqrt{(\partial x_4)^2 + (\partial x_5)^2 f(\rho; u_\Lambda) + \frac{R^2}{\rho^2 f(\rho; u_\Lambda)}}} = P_5 u_\Lambda^3. \quad (2.6)$$

This is a completely integrable system: one may simply solve for ∂x_4 and ∂x_5 and then integrate with respect to ρ . Doing so, we find

$$x_4 = \int d\rho P_4 \sqrt{\frac{\left(\frac{R}{u_\Lambda}\right)^2}{\left(\frac{\rho}{u_\Lambda}\right)^2 f(\rho; u_\Lambda) \left(\left(\frac{\rho}{u_\Lambda}\right)^6 - P_4^2 - \frac{P_5^2}{f(\rho; u_\Lambda)}\right)}} \quad (2.7)$$

$$x_5 = \int d\rho P_5 \sqrt{\frac{\left(\frac{R}{u_\Lambda}\right)^2}{\left(\frac{\rho}{u_\Lambda}\right)^2 f(\rho; u_\Lambda)^3 \left(\left(\frac{\rho}{u_\Lambda}\right)^6 - P_4^2 - \frac{P_5^2}{f(\rho; u_\Lambda)}\right)}}. \quad (2.8)$$

The above expressions represent only one branch of the solution: in the end one must match an identical branch connecting at the minimum value of $u_0 = \rho_0$. One may check explicitly that the field equations of motion arising from action (2.1) are met for the solution given by (2.7), (2.8) and (2.3).

There is a similarity to the solution for x_5 and the solution given in [9], except that a different power of ρ appears with the (also different) function f . In fact, for the case

$P_4 = 0$, we find that the minimum value of u is in fact given by u_0 , with $P_5 = \frac{u_0^3}{u_\Lambda^3} \sqrt{f(u_0; u_\Lambda)}$ which is a very similar expression to that given in [9].

The new piece of information is given by P_4 , and this changes the situation in an interesting way. First, we note that the “turn around point” for the embedding is given where ∂x_4 or ∂x_5 blow up (i.e. $u = \rho$ is not varying while both x_4 and x_5 vary allot). Note that for both x_4 and x_5 this happens at the same place: either where $f(\rho; u_\Lambda) \rightarrow 0$ or where $\left(\left(\frac{\rho}{u_\Lambda}\right)^6 - P_4^2 - \frac{P_5^2}{f(\rho; u_\Lambda)}\right) \rightarrow 0$. The question then becomes, which one goes to zero first?

To help address these questions, we first change to variables

$$\hat{\rho} = \frac{\rho}{u_\Lambda}. \tag{2.9}$$

Under this transformation we are considering where

$$\begin{aligned} f(\rho; u_\Lambda) &= f(\hat{\rho}; 1) = 0 \\ \left(\hat{\rho}^6 - P_4^2 - \frac{P_5^2}{f(\hat{\rho}; 1)}\right) &= 0. \end{aligned} \tag{2.10}$$

We can now see which one goes to 0 first: it is clearly the second line (when $P_5 \neq 0$). Imagine coming in from very large positive $\hat{\rho}$ and decreasing this value. The first line goes to zero only when $\hat{\rho} = 1$. However, in such a limit, the second line already has a zero. This is because of the f in the denominator of the last term is going to zero (from the positive side), and so at some point this will compensate for the value of $\hat{\rho}^6 - P_4^2$, and have a zero at a value of $\hat{\rho} > 1$.

The only special case is when $P_5 = 0$. When this is the case, one of the functions goes to zero at $\max\left(P_4^{\frac{1}{3}}, 1\right)$. Note that this has the peculiar feature that the endpoints of the D7 brane (a function of P_4) may not be at the same point, but none the less, the brane falls all the way to the bottom of the cigar $u = u_\Lambda$. This ceases once $|P_4| > 1$. If $|P_4| > 1$, then the embedding isn’t antipodal any more in x_5 . In the x_5, u plane, the embedding never reaches the bottom point, and so then never needs to be matched to a solution going through the origin (we will see this more clearly we plot the asymptotic separation distance as a function of P_4 and P_5).

One can check the above discussion of $u_0 = \rho_0 = \hat{\rho}_0 u_\Lambda$ simply by plotting the results. We define $\hat{\rho}_0$ by the equation

$$\left(\hat{\rho}_0^6 - P_4^2 - \frac{P_5^2}{f(\hat{\rho}_0; 1)}\right) = 0. \tag{2.11}$$

Clearly, $\hat{\rho}_0$ is a function $\hat{\rho}_0(P_4, P_5)$ and so we may plot this (we plot the largest real root), and compare it with the value 1 in figure 2. Further, we can see the special case of $P_5 = 0$ arising, and the flattening of the function that happens along the line interval $|P_4| < 1$: indeed $\max\left(P_4^{\frac{1}{3}}, 1\right)$ is the limiting value of the solution along the line $P_5 = 0$. Further, for large values of P_4 and P_5 , the value of the zero $\hat{\rho}_0$ grows as well, and so the f in the last part of the expression can be approximated by 1. This gives that the approximate value of the

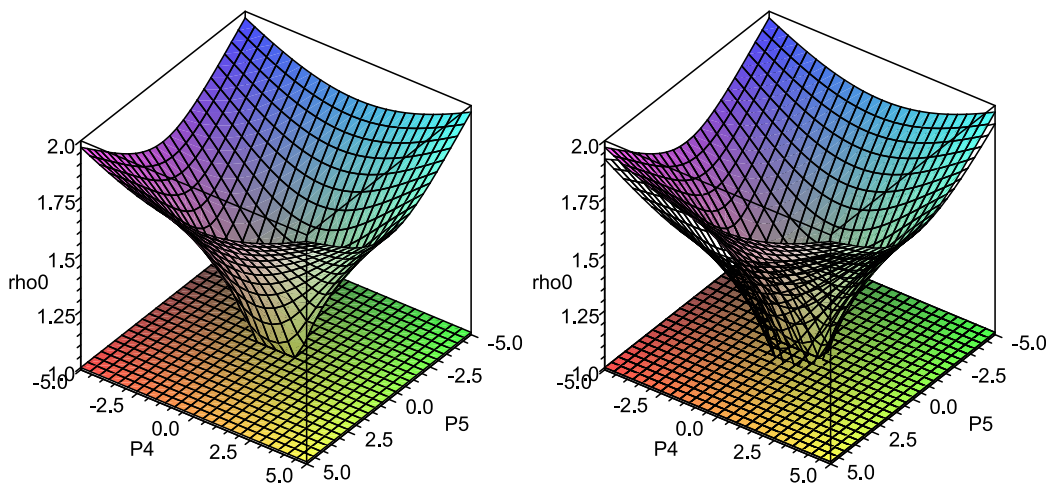


Figure 2. A plot of the largest real root, $\hat{\rho}_0(P_4, P_5) = u_0(P_4, P_5)$. Note all values are larger than 1. The wire frame in the right hand plot corresponds to the large P_i asymptote $\hat{\rho}_0(P_4, P_5) \rightarrow (P_4^2 + P_5^2)^{\frac{1}{6}}$.

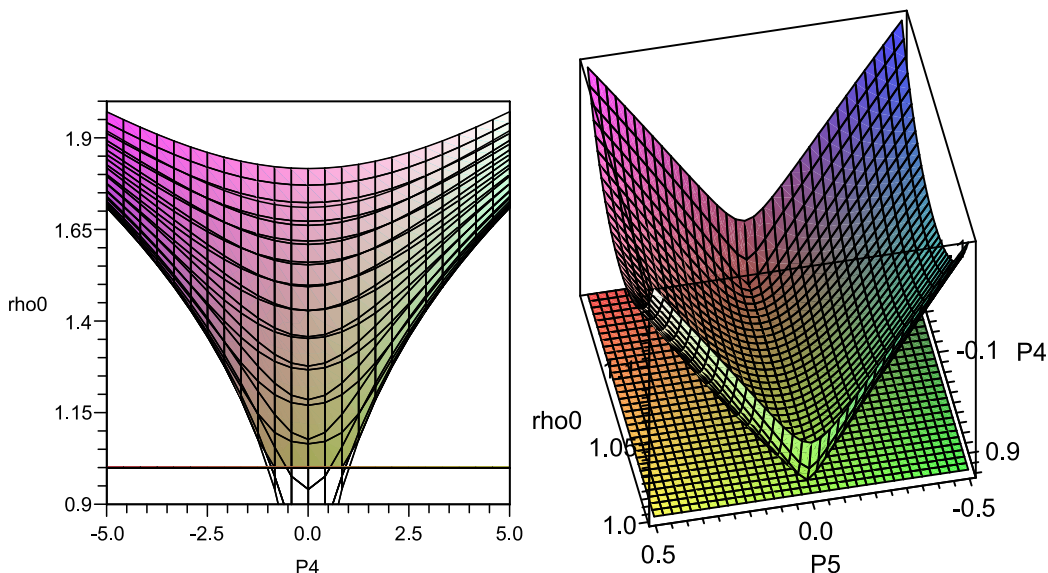


Figure 3. The left hand graph is a side view of the plot of the root of the above rational function, plotted as a function of P_4, P_5 . The black wire frame plot is the asymptote $\hat{\rho}_0 = (P_4^2 + P_5^2)^{\frac{1}{6}} = P_4^{\frac{1}{3}}$ when $P_5 = 0$. The right hand graph is a plot of $\hat{\rho}_0(P_4, P_5)$ zoomed in on the region $P_5 = 0, |P_4| < 1$. One may see that this surface is smooth on the line interval $P_5 = 0, |P_4| < 1$ except the endpoints $P_5 = 0, P_4 = \pm 1$.

zero is given by $\hat{\rho}_0 = (P_4^2 + P_5^2)^{\frac{1}{6}}$. We plot this limiting value and show that it does indeed asymptote (see figure 2). Finally, one can show that this surface exactly corresponds to the curve $\max(P_4^{\frac{1}{3}}, 1)$ along the line $P_5 = 0$ by plotting a side view (see figure 3).

One may be curious how $\hat{\rho}_0 \rightarrow 1$ as $P_5 \rightarrow 0$ on the line interval $|P_4| < 1$. Clearly, it must relax as P_5^2 , and so must be smooth around $P_5 = 0$. We plot a zoomed in version of

the plot of $\hat{\rho}_0$ and find that this is indeed the case. The only singular points on the surface (with conical singularities) are at $(P_5, P_4) = (0, \pm 1)$. See figure 3.

Now that we have found (qualitatively) the minimum value to which the brane falls, we also wish to relate the parameters P_4 and P_5 to brane separation at $u = \infty$ (in the coordinates x_4 and x_5). We will call the asymptotic separation in $\Delta x_4 = L_4$ and $\Delta x_5 = L_5$. In the end it will be these separations that we wish to consider the “boundary conditions” imposed on the branes, so that the fluctuations around these embeddings will satisfy Dirichlet boundary conditions. Given the above expressions, we see that

$$L_4 = 2R \int_{\hat{\rho}_0}^{\infty} d\hat{\rho} P_4 \sqrt{\frac{1}{\hat{\rho}^2 f(\hat{\rho}; 1) \left(\hat{\rho}^6 - P_4^2 - \frac{P_5^2}{f(\hat{\rho}; 1)} \right)}} \quad (2.12)$$

$$L_5 = 2R \int_{\hat{\rho}_0}^{\infty} d\hat{\rho} P_5 \sqrt{\frac{1}{\hat{\rho}^2 f(\hat{\rho}; 1)^3 \left(\hat{\rho}^6 - P_4^2 - \frac{P_5^2}{f(\hat{\rho}; 1)} \right)}}. \quad (2.13)$$

where the factor of 2 comes from “gluing” the second branch of the solution on. Again, finding analytic solutions to the above is problematic, but we can graph the results as a function of P_4 and P_5 , see figure 4.

We first consider the graph of L_5/R . Before making this graph, one may think that we need to be careful about finding the actual separation distance L_5 : one could have a solution that connects through smoothly the point $u = u_\Lambda$, and so the second branch actually lies displaced by $\pi R_{x_5} = \pi R$. However, the integral for L_5/R appears to have this built in. The only cases where the turn around point of the branes lies at $u_0 = u_\Lambda$ is on the interval $-1 < P_4 < 1$ and $P_5 = 0$, and so we focus on this region. While we do not offer an analytic proof, we may zoom in on this part of the graph, and be convinced that $L_5/R \rightarrow \pm\pi$ (see figure 5). One may also be convinced simply by noting that if $P_4 = P_5 = 0$, then the second branch must be glued on in antipodally after reaching $u = u_\Lambda$ to avoid a discontinuity in the tangent vector in u, x_5, x_5 space. If this is the case, we see that the integrand in the expression for L_5 must collapse to a delta function with coefficient $\pm\pi$ in the limit that $P_5 \rightarrow \pm 0$. For generic values of $\hat{\rho}$ the limit $P_5 \rightarrow 0$ sets the integrand to zero, however at $\hat{\rho} = \hat{\rho}_0$ it blows up to infinity with the integral underneath remaining constant. This is sufficient to show that the integrand goes to a delta function in $\hat{\rho}$ for the limit $P_5 \rightarrow 0$. This also explains why one misses this if one passes the limit $P_5 = 0$ under the integration: the limit implied by the integral and the limit $P_5 \rightarrow 0$ do not commute, and so one must put in the additional π of separation by hand. Further, because the values $\pm\pi$ are identified, the surface is actually continuous.

Next we consider the graph for L_4 . In figure 4 there is a divergence in L_4 around $P_5 = 0$ and $P_4 \rightarrow \pm 1$. This is easy to understand. If one looks at $P_5 = 0$ and $P_4 = 1$, the integrand goes as $\frac{1}{\hat{\rho}-1}$ around $\hat{\rho} = \hat{\rho}_0 = 1$, and so the integral is log divergent. Because L_4 blows up around $P_5 = 0, P_4 = \pm 1$ we may wish to exclude multiple wrappings of the D7 around x_4 . We further restrict the total x_4 winding to be π/R_{x_4} (half the circumference), knowing that there is another solution where the same boundary conditions are satisfied,

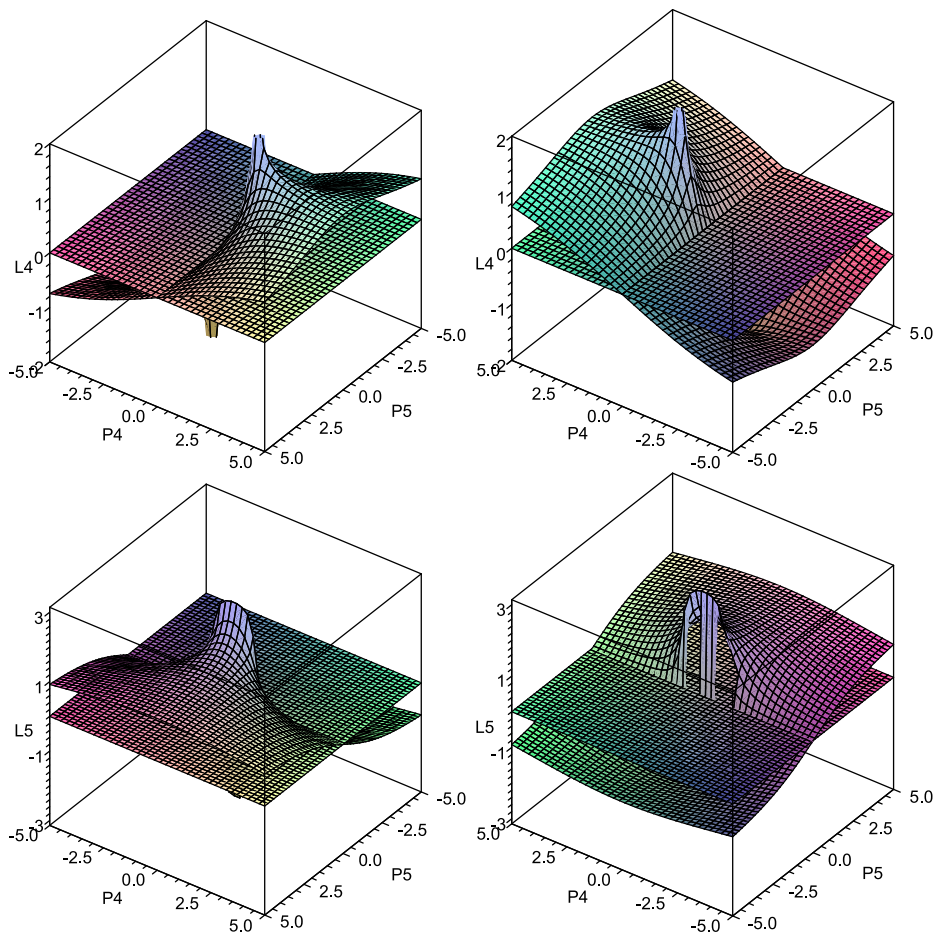


Figure 4. Plots of $L_4(P_4, P_5)/R$ and $L_5(P_4, P_5)/R$ (labeled simply L_4 and L_5 in the graphs). The view on the left gives the same perspective as earlier graphs, while the view on the right is slightly easier to see what is happening near the surface $L_4(P_4, P_5)/R = 0$ and $L_5(P_4, P_5)/R = 0$.

and less distance has been traversed by the brane. Hence, one may wish to exclude a small region around $P_5 = 0$ and $P_4 = \pm 1$ whose boundary is given by $|L_4|/R = \pi R_{x_4}/R$.

The above considerations are what lead to the diagram in figure 1.

2.1 Mesons in the model

The mesons of this model are described by strings ending on the D7 branes[28]. The high spin mesons are given by semiclassical strings which end on the D7 at the minimal value of the brane embedding u_0 , fall towards the minimum value of u_Λ and lay flat at this value and finally climb back up to meet the D7 again at u_0 . The low spin (vector) mesons are given by fluctuations of the D7 $U(N)$ gauge field strength, and the scalar mesons are given by the fluctuations of the embedding functions.

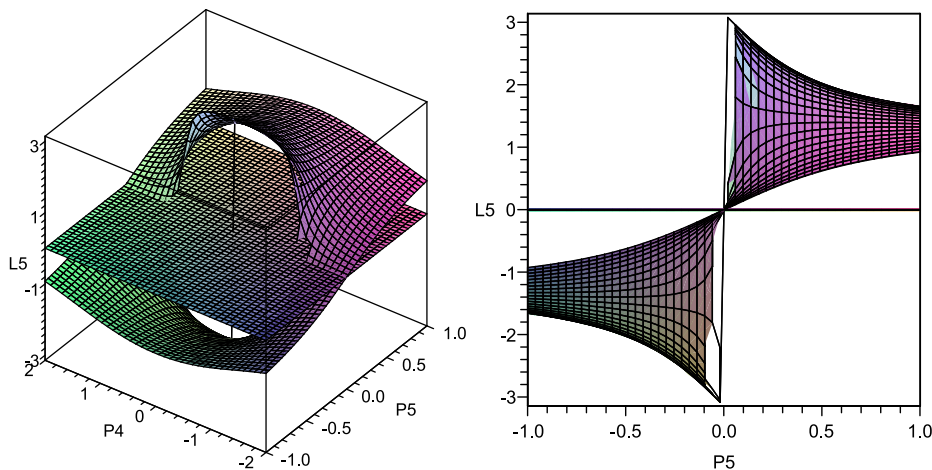


Figure 5. Plots of $L_5(P_4, P_5)/R$ zoomed in around the interval. Note that in the side view the maximum and minimum appears to approach $\pm\pi$.

To compute any of these fluctuations, we will need the pullback metric

$$\begin{aligned} ds_p^2 &= \frac{\rho}{R} \left(\eta_{\mu\nu} dx^\mu dx^\nu + \left(\partial x_4^2 + \partial x_5^2 f(\rho; u_\Lambda) + \frac{R^2}{\rho^2} \frac{1}{f(\rho; u_\Lambda)} \right) d\rho^2 + R^2 d\Omega_3^2 \right) \\ &= \frac{u_\Lambda}{R} \hat{\rho} \left(\eta_{\mu\nu} dx^\mu dx^\nu + \gamma(\hat{\rho}) \frac{R^2}{\hat{\rho}^2} d\hat{\rho}^2 + R^2 d\Omega_3^2 \right). \end{aligned} \quad (2.14)$$

where we have defined the useful function

$$\gamma(\hat{\rho}) \equiv \frac{\hat{\rho}^6}{f(\hat{\rho}; 1) \left(\hat{\rho}^6 - P_4^2 - \frac{P_5^2}{f(\hat{\rho}; 1)} \right)}. \quad (2.15)$$

For later use, we will also need

$$\exp(-\phi) \sqrt{-\det(g_{(p)ab})} = \frac{u_\Lambda^3 R}{g_s} \hat{\rho}^2 \sqrt{\gamma(\hat{\rho})} \quad (2.16)$$

and we find it convenient to use the notation

$$\frac{\partial}{\partial \rho} = \partial, \quad \frac{\partial}{\partial \hat{\rho}} = \hat{\partial} = u_\Lambda \partial, \quad \frac{\partial}{\partial x^\mu} = \partial_\mu. \quad (2.17)$$

With such an assignment, the solutions above read as

$$\hat{\partial} x_4 = RP_4 \frac{1}{\sqrt{\hat{\rho}^2 f(\hat{\rho}; 1) \left(\hat{\rho}^6 - P_4^2 - \frac{P_5^2}{f(\hat{\rho}; 1)} \right)}} = \frac{RP_4}{\hat{\rho}^4} \sqrt{\gamma(\hat{\rho})} \quad (2.18)$$

$$\hat{\partial} x_5 = RP_5 \frac{1}{\sqrt{\hat{\rho}^2 f(\hat{\rho}; 1)^3 \left(\hat{\rho}^6 - P_4^2 - \frac{P_5^2}{f(\hat{\rho}; 1)} \right)}} = \frac{RP_5}{\hat{\rho}^4 f(\hat{\rho}; 1)} \sqrt{\gamma(\hat{\rho})}. \quad (2.19)$$

2.1.1 Vector mesons

First, we compute the effective action for the fluctuations associated with the gauge field F_{ab} which we take to be only a function of $\hat{\rho}, x^\mu$ and further that components of F with indices along the sphere directions are zero. With this, we take the DBI and expand it to second order in F ,²

$$\begin{aligned} S_{D7} &= -\kappa_7 \int d^8\xi \exp(-\phi) \sqrt{-\det(g_{(p)ab} + F_{ab})} \\ &= -\kappa_7 \int d^8\xi \exp(-\phi) \sqrt{-\det(g_{(p)ab})} \\ &\quad \times \sqrt{\left(1 + g_p^{a_1 b_1} F_{a_1 b_1} + \frac{1}{2} F_{a_1 b_1} F_{a_2 b_2} \left(g_p^{a_1 b_1} g^{a_2 b_2} - g_p^{a_1 b_2} g_p^{a_2 b_1}\right) + \dots\right)} \end{aligned} \quad (2.20)$$

and now because F is antisymmetric, while g is symmetric, we find that to leading order

$$= -\kappa_7 \int d\Omega_3 \int dx^\mu d\hat{\rho} \frac{u_\Lambda^3 R}{g_s} \hat{\rho}^2 \sqrt{\gamma(\hat{\rho})} \left(1 + \frac{1}{4} F_{a_1 b_1} F_{a_2 b_2} g_p^{a_1 a_2} g_p^{b_1 b_2} + \dots\right). \quad (2.21)$$

Hence, the quadratic action we wish to consider is

$$\begin{aligned} S_{F^2} &= -\frac{\kappa_7 \Omega_3}{4g_s} \int dx^4 d\hat{\rho} u_\Lambda^3 R \hat{\rho}^2 \sqrt{\gamma(\hat{\rho})} \left(\frac{R^2}{\hat{\rho}^2 u_\Lambda^2} F_{\mu_1 \mu_2} F^{\mu_1 \mu_2} + \frac{2}{u_\Lambda^2 \gamma(\hat{\rho})} F_{\mu_1 \hat{\rho}} F^{\mu_1 \hat{\rho}}\right) \\ &= -\frac{\kappa_7 \Omega_3}{4g_s} \int dx^4 d\hat{\rho} u_\Lambda R^3 \left(\sqrt{\gamma(\hat{\rho})} F_{\mu_1 \mu_2} F^{\mu_1 \mu_2} + \frac{2\hat{\rho}^2}{R^2 \sqrt{\gamma(\hat{\rho})}} F_{\mu_1 \hat{\rho}} F^{\mu_1 \hat{\rho}}\right) \end{aligned} \quad (2.22)$$

and in the above we have used $\eta^{\mu\nu}$ to raise and lower indices.

The equations of motion following from the above action are

$$\sqrt{\gamma} \partial_\nu F^{\nu\mu} + \hat{\partial} \sqrt{\gamma} F^{\hat{\rho}\mu} = 0 \leftrightarrow \sqrt{\gamma} \partial^\nu F_{\nu\mu} + \hat{\partial} \left(\frac{\hat{\rho}^2}{R^2 \sqrt{\gamma}} F_{\hat{\rho}\mu}\right) = 0 \quad (2.23)$$

$$\partial_\mu F^{\mu\hat{\rho}} = 0 \leftrightarrow \partial^\mu F_{\mu\hat{\rho}} = 0. \quad (2.24)$$

We expand the gauge field in the following way

$$A_\mu = \sum_n B_\mu^{(n)}(x^\nu) \psi_n(\hat{\rho}), \quad A_{\hat{\rho}} = \sum_n \pi_{(n)}(x^\mu) \phi_n(\hat{\rho}). \quad (2.25)$$

We further gauge fix $\partial^\mu B_\mu^{(n)} = 0$. Under these conditions, and for the above gauge choice, we see that the equation (2.24) becomes

$$\sum_n m_n^2 \pi_n \phi_n(\hat{\rho}) - \sum_n \partial_\mu B^\mu \hat{\partial} \psi_n = \sum_n m_n^2 \phi_n(\hat{\rho}) = 0 \quad (2.26)$$

where m_n is defined by $\partial_\mu \partial^\mu B_\nu = m_n^2 B_\nu$. We see that $\phi_n = 0$ by this equation of motion except for the case where $m_n = 0$. We choose to index such a mode $m_0 = 0$. π_0 is the massless pion.

²We need not worry about the CS term because the pullback of A_6 (generated by the $D5$ background) onto the $D7$ worldvolume is zero. Note also that we are taking F to be a $U(1)$ gauge field. One may generalize this discussion to a $U(N)$ field by promoting F to a matrix, and taking a trace.

We now note that the remaining equation of motion (2.23) reads

$$\sum_n \left[\gamma^{\frac{1}{2}} \partial_\mu \partial^\mu B_{(n)}^\nu \psi_n + \hat{\partial} \left(\frac{\hat{\rho}^2}{R^2 \gamma^{\frac{1}{2}}} \hat{\partial} \psi_n \right) B_{(n)}^\nu \right] - \hat{\partial} \left(\frac{\hat{\rho}^2}{R^2 \gamma^{\frac{1}{2}}} \partial^\nu \pi_0 \phi_0 \right) = 0. \quad (2.27)$$

One can show that there are no massless normalizable modes of the vectors B_ν , and so we find that

$$\hat{\partial} \left(\frac{\hat{\rho}^2}{R^2 \gamma^{\frac{1}{2}}} \partial^\nu \pi_0 \phi_0 \right) = 0 \rightarrow \phi_0 \propto \frac{\gamma^{\frac{1}{2}}}{\hat{\rho}^2}. \quad (2.28)$$

Thus, we find that the eigenvalue problem for the ψ_n reduces to

$$\frac{1}{\gamma^{\frac{1}{2}}} \hat{\partial} \left(\frac{\hat{\rho}^2}{\gamma^{\frac{1}{2}}} \hat{\partial} \psi_n \right) = -M_{A,n}^2 \psi_n \quad (2.29)$$

where the 4D mass is given by $m_{A,n} = \frac{M_{A,n}}{R}$.

Unfortunately, the eigenvalue problem for the fluctuations of the embedding coordinates are much more involved because we do not have a good set of orthogonal coordinates to the brane. However, we will study these in two special cases below.

3 Large $u_0 \gg u_\Lambda$ limit

In this section, we consider the limit where $u_0 \gg u_\Lambda$. This limit is the same as the extremal limit of the background because $f(u; u_\Lambda)$ can be approximated by $f(u; u_\Lambda) = 1$. As mentioned in the introduction this case makes sense also quantum mechanically. In fact it is similar to the cases studied in [29]. In such a limit the periodic identification of x_4 and x_5 now both become arbitrary, and further there is an additional $SO(2)$ symmetry rotating the x_4, x_5 plane, which the solutions will transform under in a simple way. To consider the limit $u_0 \gg u_\Lambda$, we cannot take a strict $u_\Lambda \rightarrow 0$ limit of equations (2.5) and (2.6) because this would scale the right hand side of these equations to zero (when they should be constants). Therefore, we absorb the u_Λ^3 into P_i , via $p_i \equiv u_\Lambda^3 P_i$ (the parameters p_i have units). One may think of this as a scaling where $u_\Lambda \rightarrow 0$ while $P_i \rightarrow \infty$ with $p_i = u_\Lambda^3 P_i$ remaining fixed. This is connected to the fact that for large P_i the solution is in a regime where $u_0 \gg u_\Lambda$.

We consider equations (2.5) and (2.6) with the above substitutions and set $u_\Lambda = 0$ and find

$$\frac{\rho^3 \partial x_4}{\sqrt{(\partial x_4)^2 + (\partial x_5)^2 + \frac{R^2}{\rho^2}}} = p_4 \quad (3.1)$$

$$\frac{\rho^3 \partial x_5}{\sqrt{(\partial x_4)^2 + (\partial x_5)^2 + \frac{R^2}{\rho^2}}} = p_5. \quad (3.2)$$

As before, we solve for ∂x_4 and ∂x_5 , and find

$$x_4 = \int d\rho R p_4 \sqrt{\frac{1}{\rho^2 (\rho^6 - p_4^2 - p_5^2)}} = \frac{1}{3} \frac{R p_4 \arcsin\left(\frac{\sqrt{p_4^2 + p_5^2}}{\rho^3}\right)}{\sqrt{p_4^2 + p_5^2}} + x_{4,0} \quad (3.3)$$

$$x_5 = \int d\rho R p_5 \sqrt{\frac{1}{\rho^2 (\rho^6 - p_4^2 - p_5^2)}} = \frac{1}{3} \frac{R p_5 \arcsin\left(\frac{\sqrt{p_4^2 + p_5^2}}{\rho^3}\right)}{\sqrt{p_4^2 + p_5^2}} + x_{5,0}. \quad (3.4)$$

where the constants $x_{4,0}$ and $x_{5,0}$ can be fixed to 0 by translation invariance in x_4 and x_5 (again, the above only represents 1 branch of the solution and must be glued on to another branch). This gives simple expressions for L_4 and L_5

$$\begin{aligned} L_4 &= \frac{R p_4 \pi}{3 \sqrt{p_4^2 + p_5^2}} \\ L_5 &= \frac{R p_5 \pi}{3 \sqrt{p_4^2 + p_5^2}}. \end{aligned} \quad (3.5)$$

Further, we should note that this gives that

$$L_4^2 + L_5^2 = \frac{R^2 \pi^2}{9}. \quad (3.6)$$

In the x_4, x_5 plane, the ends of the D7 brane have a fixed asymptotic separation (not including the warp factor); similar behavior was found in [19] for D5 brane embeddings. This gives that L_4 and L_5 do not parameterize the 2 dimensional class of solutions that we have. We can, however, use $\rho_0 = u_0 = (p_4^2 + p_5^2)^{\frac{1}{6}}$ and the unit vector defining the separation direction $L_4/L_5 = p_4/p_5$ as the two physical quantities. Note that one can take fixed L_4 and L_5 while varying u_0 simply by rescaling p_4 and p_5 by the same factor.

Before turning to a discussion of these embeddings, we note some general points about how to find the scaling of u_0 with various L_i in the problem. We note that in the extremal limit, the action becomes

$$S_{D7} = \frac{\kappa_7 V_3 V_4}{g_s} \int d\rho u^3 \sqrt{(\partial x_4)^2 + (\partial x_5)^2 + \frac{R^2 \partial u^2}{u^2}} \quad (3.7)$$

where in the above we have not fixed $u = \rho$ as a gauge choice. We note that there is a Lie point symmetry (for more on Lie point symmetries, see [30]) of the equations of motion following from the above action. Namely, if we take

$$u \rightarrow C \times u \quad (3.8)$$

the action scales as

$$S_{D7} \rightarrow C^3 S_{D7}. \quad (3.9)$$

This is clearly a symmetry of the solution space of the equations of motion. The above symmetry is therefore a local map from solutions to solutions, the definition of a Lie point symmetry.

One could further scale the embedding coordinates $x^\mu(\xi) \rightarrow C^{n_\mu} x^\mu(\xi)$ (no summation) if one wishes (this rescales the effective V_4) and possibly promote the above symmetry to a Noether symmetry, however, we will not do this here.³ Note that in such a scaling, we have not rescaled x_4 or x_5 . Therefore, when applying this symmetry to the space of solutions, we know that $u_0 \rightarrow C \times u_0$ however, L_4 and L_5 do not scale at all (as they are related to the asymptotic separation of x_4 and x_5). This further accounts for the same behavior for the D5 embeddings found in [19].

One can use such arguments to get the correct behavior in a host of situations. Of particular interest is the situation where the metric is of the form $g_{ij}(u)dx^i dx^j + f(u) \times (du^2 + u^2 d\Omega_M^2)$ where all metric components along the i, j directions are functions of u only, and $d\Omega_M^2$ is the metric of some compact space spanned by coordinates θ^i . We further assume that the dilaton is a function only of u . The reduced one dimensional Lagrangian with $x^i = \xi^i$ and $\theta^i = \theta^i(r)$ will always be of the form $G(u)\sqrt{(1 + u^2 d\Omega_M^2)}$ where now all of the ds in the metric $d\Omega_M^2$ are to be read as derivatives with respect to u . In such a situation, $u \rightarrow C \times u$ is a Lie point symmetry of the action if $G(C \times u) = G(u) \times C^\Delta$, i.e. $G(u) = u^\Delta$. This covers most extremal brane type embeddings. Further, such behavior is intuitive for “flat” type embeddings of the probe brane in supersymmetric situations. For a supersymmetric situation, the probe brane does not “see” the background it is in, and simply goes along a straight path (straight in the sense of the flat geometry with no backreacted branes). Therefore, the angular separation is always a “north pole/south pole” type (at least asymptotically), and will not depend on u_0 at all. As an example, see the discussion of [4] (equation (8)). Of course the angular separation may be changed by some constant if there is a conical singularity at the origin of the transverse space (at $u = 0$), as in the more recent calculation [31] (see the last paragraph of section 3), however there should still be no dependence on u_0 .

We can explore such possibilities in general. Consider a situation where the metric is of the form $C_1 r^n dx^i dx^j \eta_{ij} + C_2 r^m dr^2 + C_3 r^{m+2} d\Omega^2$, and the dilaton is of the form $\exp(\phi) \propto r^q$. If one reduces the the DBI action to a one dimensional action via $x^i = x^i(r), \theta^i = \theta^i(r)$ (with an appropriate number of static gauge coordinates), one will always have the Lie point symmetry $r \rightarrow C \times r, x^i \rightarrow C^{\frac{m-n+2}{2}} x^i, \theta^i \rightarrow \theta^i$. In such a situation, the asymptotic separation in the x^i is $\Delta x^i \propto u_0^{\frac{m-n+2}{2}}$, and the angular separation $\Delta\theta^i = \text{constant}$. For example in the case of the extremal Sakai-Sugimoto model [7, 8] $n = 3/2, m = -3/2$ and so $\Delta x^4 \propto u_0^{-\frac{1}{2}} R^{\frac{3}{2}}$, where we have used R to make the correct units. This answer is indeed correct [16] (see equation (2.18) of this work).

Our situation is somewhat special, where both the sphere and the flat space component have the same warp factor up to a constant. This is the reason that in our extremal case, L_4 and L_5 do not depend at all on u_0 . It is a statement that a pure rescaling in u is a Lie

³This is because the particular form of this symmetry is dependent on the fact that at least 4 of the fields x^μ, x^4, x^5 are along the world volume of the D7 and aligning them to be the first 4 x^μ via a Lorentz transformation, and then further gauge fixing these to be ξ^μ . Thus, if we truly wanted to extend the above symmetry to a Noether symmetry, we would need to include some combination of coordinate transformations and Lorentz symmetry too, which we do not wish to consider here.

point symmetry, without requiring extra rescalings of the functions x^i . Further, in such situations, the boundary conditions are not affected by varying u_0 . Therefore, one may expect such a mode to be normalizable, and correspond to a massless mode. One usually thinks of such a mode as a Goldstone boson of some spontaneously broken symmetry. Here, the symmetry is the Lie point symmetry promoted to a full Noether symmetry, as discussed in the footnote earlier. This is a full (non linear) symmetry of the DBI action. It would be interesting to see what the symmetry of the DBI action corresponds to on the field theory side.

We now turn back to the embeddings at hand. Note that using the $SO(2)$ symmetry of the background (mixing x_4 and x_5), one may rotate and translate to a frame where $x_4 = 0$, and further, $x_5(u) \in (-\frac{R\pi}{6} \dots \frac{R\pi}{6})$. Such a frame change will mix any periodic identifications one has made in x_4 and x_5 (by a slant identification “ τ ”), however, the local physics of the embedding will not be dependent on such considerations. Therefore, the point $x_5 = 0$ corresponds to where the embedding has reached u_0 . Therefore, we may summarize the embedding as

$$u(x_5) = \left(\frac{p_5}{\sin\left(\frac{3(x_5 + \frac{R\pi}{6})}{R}\right)} \right)^{\frac{1}{3}}. \tag{3.10}$$

This is suggestive of a change of variables. We make the change

$$y = u^3 \sin\left(\frac{3(x_5 + \frac{R\pi}{6})}{R}\right) \tag{3.11}$$

$$v = u^3 \cos\left(\frac{3(x_5 + \frac{R\pi}{6})}{R}\right). \tag{3.12}$$

In these coordinates, the metric becomes

$$ds^2 = \frac{(y^2 + v^2)^{\frac{1}{6}}}{R} (\eta_{\mu\nu} dx^\mu dx^\nu + dx_4^2) + \frac{R}{9(y^2 + v^2)^{\frac{5}{6}}} (dy^2 + dv^2) + R(y^2 + v^2)^{\frac{1}{6}} d\Omega_3^2. \tag{3.13}$$

We change to “7 brane frame” via

$$G_{IJ} = \exp\left(-\phi \frac{2}{8}\right) g_{IJ}. \tag{3.14}$$

Changing frame in this way gives that $\sqrt{\det G_p} = \sqrt{\det g_p} \exp(-\phi)$ where G_p is the pull-back of the above G to the D7 world volume. In this frame

$$\frac{g_s^{\frac{1}{4}}}{R^{\frac{1}{4}}} ds_G^2 = \frac{(y^2 + v^2)^{\frac{1}{8}}}{R} (\eta_{\mu\nu} dx^\mu dx^\nu + dx_4^2) + \frac{R}{9(y^2 + v^2)^{\frac{7}{8}}} (dy^2 + dv^2) + R(y^2 + v^2)^{\frac{1}{8}} d\Omega_3^2. \tag{3.15}$$

The embedding of the D7 is now given by $y = p_5 = u_0^3, x_4 = 0$. This gives the pullback metric to be

$$\frac{g_s^{\frac{1}{4}}}{R^{\frac{1}{4}}} ds_G^2 = \frac{(u_0^6 + v^2)^{\frac{1}{8}}}{R} (\eta_{\mu\nu} dx^\mu dx^\nu) + \frac{R}{9(u_0^6 + v^2)^{\frac{7}{8}}} (dv^2) + R(u_0^6 + v^2)^{\frac{1}{8}} d\Omega_3^2. \quad (3.16)$$

One can now see why $y = u_0^3$ is a good embedding for any u_0 : the determinant of the above metric does not depend on the warp factors $(u_0^6 + v^2)$! We will see the solution associated with shifting u_0 in the linearized equations of motion, which we will study in the next section. We now add a word of caution. The above symmetry scaling u_0 to different values is only a classical symmetry. This may not be true quantum mechanically, in analogy with the expectations for u_Λ expressed in section 1 [20].

3.1 Scalar mesons

We now turn to the fluctuations of the above embedding. To do so, we expand the fields as $y = u_0^3 + w(v, x^\mu), x_4 = 0 + x_4(v, x^\mu)$. Therefore, we find

$$\begin{aligned} \frac{g_s^{\frac{1}{4}}}{R^{\frac{1}{4}}} ds_G^2 &= \frac{((u_0^3 + w)^2 + v^2)^{\frac{1}{8}}}{R} (dx^\mu dx_\mu) + \frac{R}{9((u_0^3 + w)^2 + v^2)^{\frac{7}{8}}} (dv^2) \\ &\quad + R((u_0^3 + w)^2 + v^2)^{\frac{1}{8}} d\Omega_3^2 \\ &\quad + \frac{R}{9(u_0^6 + v^2)^{\frac{7}{8}}} (\partial_v w dv + \partial_\mu w dx^\mu)^2 + \frac{(u_0^6 + v^2)^{\frac{1}{8}}}{R} (\partial_v x_4 dv + \partial_\mu x_4 dx^\mu)^2. \end{aligned} \quad (3.17)$$

We wish to expand $\det(G_p)$ to second order in w and x_4 . With the above parametrization, this is now easy, as we may think of the third line as a perturbation of a metric given by the first line. Therefore, we define

$$\begin{aligned} \frac{g_s^{\frac{1}{4}}}{R^{\frac{1}{4}}} ds_0^2 &= \frac{((u_0^3 + w)^2 + v^2)^{\frac{1}{8}}}{R} (dx^\mu dx_\mu) + \frac{R}{9((u_0^3 + w)^2 + v^2)^{\frac{7}{8}}} (dv^2) \\ &\quad + R((u_0^3 + w)^2 + v^2)^{\frac{1}{8}} d\Omega_3^2 \end{aligned} \quad (3.18)$$

and use this to define a metric G_p . Now, to leading order, the expanded metric

$$\det(G_p + h) = \det(G_p) (1 + G_p^{a_1 a_2} h_{a_1 a_2}). \quad (3.19)$$

In the second term of the above, we may substitute $w = 0$ into the metric g_p as h is already second order in w and x_4 . Further, $\det(g_p)$ does not depend on w or x_4 , and so there is no need to expand further. We therefore find that, to second order

$$\begin{aligned} \int d\Omega_3 \sqrt{\det(G_p)} &= \Omega_3 \frac{R}{3g_s} \left(1 + \frac{1}{2} \partial_\mu x_4 \partial^\mu x_4 + \frac{9(u_0^6 + v^2)}{R^2} \frac{1}{2} (\partial_v x_4)^2 \right. \\ &\quad \left. + \frac{R^2}{9(u_0^6 + v^2)} \frac{1}{2} \partial_\mu w \partial^\mu w + \frac{1}{2} (\partial_v w)^2 \right). \end{aligned} \quad (3.20)$$

The second order action we wish to consider is therefore

$$S = -\frac{\kappa_7 R \Omega_3}{g_s} \int dv d^4x \left(\frac{\zeta^{-1}}{9} \frac{1}{2} \partial_\mu w \partial^\mu w + \frac{1}{2} (\partial_v w)^2 + \frac{1}{2} \partial_\mu x_4 \partial^\mu x_4 + 9\zeta \frac{1}{2} (\partial_v x_4)^2 \right)$$

with

$$\zeta \equiv \frac{u_0^6 + v^2}{R^2}. \quad (3.21)$$

The above action has positive definite Hamiltonian, so we expect the embedding to be stable.

The eigenvalue problem we wish to satisfy is the following

$$\partial_V (9(1+V^2) \partial_V \psi_{x,M_x}) = -M_x^2 \psi_{x,M_x}(V) \quad (3.22)$$

$$9(1+V^2) \partial_V^2 \psi_{w,M_w}(V) = -M_w^2 \psi_{w,M_w}(V). \quad (3.23)$$

where the 4D masses are given by $m_i = \frac{M_i}{R}$ and we have defined $V = \frac{v}{u_0^3}$. These have the general solutions

$$\begin{aligned} \psi_{x,M_x}(V) = & C_{1,x} P \left(\frac{\sqrt{9-4M_x^2}}{6} - \frac{1}{2}; -iV \right) + \\ & + C_{2,x} Q \left(\frac{\sqrt{9-4M_x^2}}{6} - \frac{1}{2}; -iV \right) \end{aligned} \quad (3.24)$$

$$\begin{aligned} \psi_{w,M_w}(V) = & C_{1,w} (1+V^2) {}_2F_1 \left(\frac{3}{4} + \frac{\sqrt{9-4M_w^2}}{12}, \frac{3}{4} - \frac{\sqrt{9-4M_w^2}}{12}; \frac{1}{2}; -V^2 \right) \\ & + C_{2,w} V (1+V^2) {}_2F_1 \left(\frac{5}{4} + \frac{\sqrt{9-4M_w^2}}{12}, \frac{5}{4} - \frac{\sqrt{9-4M_w^2}}{12}; \frac{3}{2}; -V^2 \right) \end{aligned} \quad (3.25)$$

where P and Q are Legendre functions, and ${}_2F_1$ is the hypergeometric function. There are possible bound states in the regime

$$0 \leq m_{x,w} = \frac{M_{x,w}}{R} \leq \frac{3}{2} \frac{1}{R}. \quad (3.26)$$

Curiously, we will find this to be true in the next section as well, where we consider an embedding into the near extremal background.

We now change the eigenvalue problem to Schödinger form to analyze the above differential equations. We do so by changing coordinates and variables

$$\begin{aligned} V &= \sinh(K) \\ \psi_{w,M_w}(K) &= \sqrt{\cosh(K)} \Psi_{w,M_w}(K) \\ \psi_{x,M_x}(K) &= \frac{1}{\sqrt{\cosh(K)}} \Psi_{x,M_x}(K). \end{aligned} \quad (3.27)$$

This brings the equations to the following form

$$\partial_K^2 \Psi_{w,M_w}(K) - \left(\frac{1}{4} - \frac{3}{4} \frac{1}{\cosh(K)^2} \right) \Psi_{w,M_w}(K) = -\frac{1}{9} M_w^2 \Psi_{w,M_w}(K) \quad (3.28)$$

$$\partial_K^2 \Psi_{x,M_x}(K) - \left(\frac{1}{4} + \frac{1}{4} \frac{1}{\cosh(K)^2} \right) \Psi_{x,M_x}(K) = -\frac{1}{9} M_x^2 \Psi_{x,M_x}(K). \quad (3.29)$$

The second line clearly has no normalizable bound states, where as the first at least has the possibility. In fact, the above set of differential equations is *exactly* the same as those encountered in the next section, with a simple modification.

In the next section we show that there is only one bound state for the equation of the first type above, and in fact this is the the $M_w = 0$ mode anticipated by the discussion above. For $M_w = 0$, we find

$$\Psi_{w,M_w=0}(K) = \frac{C_{1,w}}{\sqrt{\cosh(K)}} + \frac{C_{2,w} \sinh(K)}{\sqrt{\cosh(K)}}. \quad (3.30)$$

The first is clearly normalizable, where the second is clearly non normalizable. Further, taking the normalizable solution, we find that the profile in $\psi_{w,M_w=0} = C_{1,w}$, exactly corresponding to shifts in the definition of u_0 . We will fully analyze the above type of differential equations in the next section.

3.2 Vector mesons

We now analyze the fluctuations of the world volume vector gauge field. As in the previous section, we find that

$$= -\kappa_7 \int d\Omega_3 \int dx^\mu dv e^{-\phi} \sqrt{g_p} \left(1 + \frac{1}{4} F_{a_1 b_1} F_{a_2 b_2} g_p^{a_1 a_2} g_p^{b_1 b_2} + \dots \right). \quad (3.31)$$

which for this case gives

$$S = -\kappa_7 \Omega_3 \int dx^\mu dv \frac{R}{g_s} \left(1 + \frac{1}{4} \frac{g_s^{\frac{1}{2}} R^{\frac{3}{2}}}{(u_0^6 + v^2)^{\frac{1}{4}}} F_{\mu\nu} F^{\mu\nu} + \frac{1}{2} \frac{9g_s^{\frac{1}{2}} (u_0^6 + v^2)^{\frac{3}{4}}}{R^{\frac{1}{2}}} F_{\mu\nu} F^{\mu\nu} + \dots \right) \quad (3.32)$$

where we now use $\eta^{\mu\nu}$ to raise and lower indices. The equations of motion read

$$R^2 \partial^\mu F_{\mu\nu} + (u_0^6 + v^2)^{\frac{1}{4}} \partial_\nu \left((u_0^6 + v^2)^{\frac{3}{4}} F_{\nu\nu} \right) = 0 \quad (3.33)$$

$$\partial^\mu F_{\mu\nu} = 0. \quad (3.34)$$

As before we expand

$$A_\mu = \sum_n B_\mu^{(n)}(x) \psi_n(v), \quad A_\nu = \sum_n \pi_n(x) \phi_n(v) \quad (3.35)$$

and gauge fix $\partial^\mu B_\mu = 0$ to find

$$\sum_n R^2 \partial^\mu \partial_\mu B_\nu^{(n)} \psi_n + (u_0^6 + v^2)^{\frac{1}{4}} \partial_\nu \left((u_0^6 + v^2)^{\frac{3}{4}} \partial_\nu \psi_n \right) B_\nu^{(n)} = 0 \quad (3.36)$$

$$\partial_\nu \left((u_0^6 + v^2)^{\frac{3}{4}} \partial_\nu \pi_0 \phi_0 \right) = 0 \rightarrow \phi_0 \propto \frac{1}{(u_0^6 + v^2)^{\frac{3}{4}}}. \quad (3.37)$$

and for $n \neq 0$, $\phi_n = 0$.

We may change the ψ_n equations to Schrödinger form via

$$\frac{v}{u_0^3} = \sinh(K)$$

$$\psi_{(n)}(K) = \frac{1}{(\cosh(K))^{\frac{1}{4}}} \Psi_n \tag{3.38}$$

and taking $\partial^\mu \partial_\mu B^{(n)} = m_n^2 B^{(n)} \equiv \frac{M_n^2}{R^2} B^{(n)}$ we find

$$\partial_K^2 \Psi(K) - \frac{1}{144} \Psi(K) \left(9 + \frac{27}{\cosh(K)^2} \right) = -\frac{1}{9} M_n^2 \Psi(K). \tag{3.39}$$

This obviously has no normalizable modes. This means that the only 4D meson from this sector is the massless pion π_0 . We will see the same phenomena in the next section.

4 A simple antipodal embedding

In this section we will be concerned with the antipodal embedding $P_4 = 0, P_5 = 0$. This is the rare exception when we have an analytic solution that comes into the region $u \sim u_\Lambda$. We will find it convenient to start with the z coordinates introduced earlier

$$u^2 = u_\Lambda^2 + z^2. \tag{4.1}$$

In these variables, the metric reads

$$ds^2 = \frac{\sqrt{u_\Lambda^2 + z^2}}{R} (\eta_{\mu\nu} dx^\mu dx^\nu + dx_4^2) + R \sqrt{u_\Lambda^2 + z^2} d\Omega_3^2 + \frac{R}{\sqrt{u_\Lambda^2 + z^2}} \left(dz^2 + z^2 \frac{dx_5^2}{R^2} \right) \tag{4.2}$$

and we make the following coordinate change

$$w \equiv z \sin\left(\frac{x_5}{R}\right) \tag{4.3}$$

$$v \equiv z \cos\left(\frac{x_5}{R}\right) \tag{4.4}$$

so that

$$ds^2 = \frac{\sqrt{u_\Lambda^2 + z^2}}{R} (\eta_{\mu\nu} dx^\mu dx^\nu + dx_4^2) + R \sqrt{u_\Lambda^2 + z^2} d\Omega_3^2 + \frac{R}{\sqrt{u_\Lambda^2 + z^2}} (dw^2 + dv^2). \tag{4.5}$$

Now, the solution to the embedding reads $x_4(v) = w(v) = 0$ (we will use v as the world volume coordinate).

4.1 Scalar mesons

We now expand the action to quadratic order in $x_4(v, x^\mu), w(v, x^\mu)$. This is most easily accomplished by going to a “seven brane” frame

$$G_{IJ} = \exp\left(-\phi \frac{2}{8}\right) g_{IJ}. \tag{4.6}$$

Changing frame in this way gives that $\sqrt{\det G_p} = \sqrt{\det g_p} \exp(-\phi)$ where G_p is the pull-back of the above G to the D7 world volume. We first expand the modified line element to second order in fluctuating fields x_4 and w , and we find

$$\begin{aligned}
 g_s^{\frac{1}{4}} ds_G^2 &= \zeta^{\frac{3}{8}} \eta_{\mu\nu} dx^\mu dx^\nu + R^2 \zeta^{\frac{3}{8}} d\Omega_3^2 + \zeta^{-\frac{5}{8}} dv^2 \\
 &+ \zeta^{\frac{3}{8}} (\partial_\nu x_4 dv + \partial_\mu x_4 dx^\mu)^2 + \zeta^{-\frac{5}{8}} (\partial_\nu w dv + \partial_\mu w dx^\mu)^2 \\
 &+ \frac{3}{8} \zeta^{-\frac{5}{8}} \frac{w^2}{R^2} \eta_{\mu\nu} dx^\mu dx^\nu + R^2 \frac{3}{8} \zeta^{-\frac{5}{8}} \frac{w^2}{R^2} d\Omega_3^2 - \frac{5}{8} \zeta^{-\frac{13}{8}} \frac{w^2}{R^2} dv^2 + \dots
 \end{aligned} \tag{4.7}$$

with

$$\zeta \equiv \frac{u_\Lambda^2 + v^2}{R^2}. \tag{4.8}$$

Note that the ζ defined in this section is different than the ζ defined in the last section.

Next, we expand the action to second order and find

$$\begin{aligned}
 \int d^4 x^\mu dv d\Omega_3 \sqrt{-G_p} &= \Omega_3 \int d^4 x^\mu dv \zeta \left[1 + \frac{1}{2} \partial_\mu x_4 \partial^\mu x_4 + \frac{1}{2} \zeta (\partial_\nu x_4)^2 \right. \\
 &\left. + \frac{1}{2} \zeta^{-1} \partial_\mu w \partial^\mu w + \frac{1}{2} (\partial_\nu w)^2 + \frac{1}{2} \frac{2}{R^2} w^2 \right]
 \end{aligned} \tag{4.9}$$

which has positive definite hamiltonian, and so we expect that this embedding is stable.

The proper eigenvalue problem is

$$\begin{aligned}
 \zeta^{-1} \partial_\nu (\zeta^2 \partial_\nu \psi_{x,m_x}(v)) &= -\frac{M_x^2}{R^2} \psi_{x,m_x}(v) \\
 \partial_\nu (\zeta \partial_\nu \psi_{w,m_w}(v)) &= \left(\frac{2}{R^2} - \frac{M_w^2}{R^2} \right) \psi_{w,m_w}
 \end{aligned} \tag{4.10}$$

where the 4D masses are $m_x = \frac{M_x}{R}$ and $m_w = \frac{M_w}{R}$. The solution to these are the following

$$\begin{aligned}
 \psi_{x,M_x}(V) &= C_{x,1} {}_2F_1 \left(\frac{3}{4} - \frac{\sqrt{9-4M_x^2}}{4}, \frac{3}{4} + \frac{\sqrt{9-4M_x^2}}{4}; \frac{1}{2}; -V^2 \right) \\
 &+ C_{x,2} V {}_2F_1 \left(\frac{5}{4} - \frac{\sqrt{9-4M_x^2}}{4}, \frac{5}{4} + \frac{\sqrt{9-4M_x^2}}{4}; \frac{3}{2}; -V^2 \right)
 \end{aligned} \tag{4.11}$$

$$\begin{aligned}
 \psi_{w,M_w}(V) &= C_{w,1} P \left(\frac{\sqrt{9-4M_w^2}}{2} - \frac{1}{2}; -iV \right) \\
 &+ C_{w,2} Q \left(\frac{\sqrt{9-4M_w^2}}{2} - \frac{1}{2}; -iV \right)
 \end{aligned} \tag{4.12}$$

where

$$V = \frac{v}{u_\Lambda} \tag{4.13}$$

and ${}_2F_1$ is the hypergeometric series, and P and Q are Legendre functions. Note again that the definition of the above V differs from the last section.

There are possible bound states in the range

$$0 \leq m_{x,w} = \frac{M_{x,w}}{R} \leq \frac{3}{2} \frac{1}{R}. \quad (4.14)$$

If m_x or m_w exceed this range of values, the indices of the above functions become complex. One can show that around $V = \infty$ these go as appropriately normalized plane wave solutions, and so represent a continuum of states. This corresponds to a mass scale at which the scalar mesons may no longer be considered 4 dimensional.

We expect that the indices of the hypergeometric equation being integers is special, and we find that in the case $M_x = \sqrt{2}$ that

$$\psi_{x,M_x=\sqrt{2}}(V) = \frac{C_{x,1} + C_{x,2}V}{V^2 + 1}. \quad (4.15)$$

In such a case we see that $C_{x,2} = 0$ is a normalizable solution. We will now give an argument that this is the only bound state of the above eigenvalue equations.

We will change the one dimensional problem in hand to Schrödinger form. To do so, we take the change of variables and functions

$$V = \sinh(K) \quad (4.16)$$

$$\psi_{w,M_w}(K) = \frac{\Psi_{w,M_w}(K)}{\sqrt{\cosh(K)}} \quad (4.17)$$

$$\psi_{x,M_x}(K) = \frac{\Psi_{x,M_x}(K)}{(\cosh(K))^{\frac{3}{2}}}. \quad (4.18)$$

Then, the equations above become

$$\frac{\partial^2}{\partial K^2} \Psi_{w,M_w}(K) - \left(\frac{9}{4} + \frac{1}{4} \frac{1}{\cosh(K)^2} \right) \Psi_{w,M_w}(K) = -M_w^2 \Psi_{w,M_w}(K) \quad (4.19)$$

$$\frac{\partial^2}{\partial K^2} \Psi_{x,M_x}(K) - \left(\frac{9}{4} - \frac{3}{4} \frac{1}{\cosh(K)^2} \right) \Psi_{x,M_x}(K) = -M_x^2 \Psi_{x,M_x}(K). \quad (4.20)$$

In the above problem, we are looking for bound states whose energy is interpreted as $E = M_i^2$. Clearly there are no bound states for the potential of the first kind (it is a hill, rather than a well). In the second case, there is at least the possibility that there are bound states. Using the WKB approximation, we take

$$n = -\frac{1}{2} + \frac{1}{\pi} \int_{-\cosh^{-1}\left(\frac{3}{\sqrt{-12M_x^2+27}}\right)}^{\cosh^{-1}\left(\frac{3}{\sqrt{-12M_x^2+27}}\right)} dK \sqrt{M_x^2 - \frac{9}{4} + \frac{3}{4} \frac{1}{\cosh(K)^2}}. \quad (4.21)$$

There is a bound state when n is an integer. Clearly $\sqrt{\frac{3}{2}} < M_x < \sqrt{\frac{9}{4}}$ by considering the maximum and minimum of the potential, and so we plot the above function in this range in figure 6. The plot of n crosses an integer value only at $n = 0$. This crossing is close to the exact solution of $M_x = \sqrt{2}$, but not precise. We may expect this low level of accuracy for the least energetic bound state, but generically, the accuracy of the WKB approximation

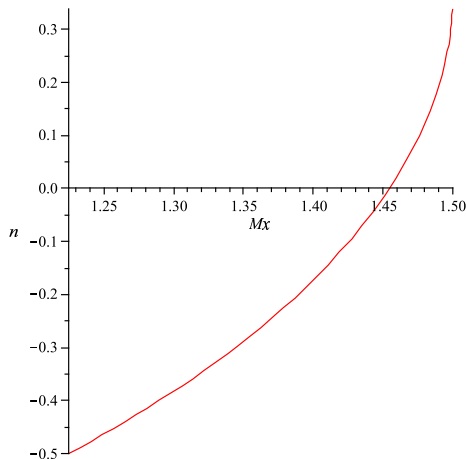


Figure 6. Plot of $n(M_x)$. Note that the only integer solution is $n = 0$, and that this approximates the known solution of $M_x = \sqrt{2}$.

is improved for higher energy bound states. Therefore, we trust that there are no other bound state solutions.

One further note is in order. For the above configuration, there is no scaling symmetry of the DBI action (as there was in the last section). Therefore, it seems plausible that the above mode is a pseudo goldstone mode associated with the scaling symmetry. Because the symmetry is not exact (due to the function f), the mass is lifted from 0. It would be interesting to find a way to track the mode from small to large values of u_0/u_Λ and see if this is indeed the case. This would further track from being a pure w excitation (when $u_0 \gg u_\Lambda$, as in the last section) to being a pure x_4 excitation (for $u_0 = u_\Lambda$, in this section). Finding the correct linear combination that was a bound 4D state, and diagonalized the mass matrix in the general case would be instructive.

4.2 Vector mesons

As in the previous section, we find that

$$= -\kappa_7 \int d\Omega_3 \int dx^\mu dv e^{-\phi} \sqrt{g_p} \left(1 + \frac{1}{4} F_{a_1 b_1} F_{a_2 b_2} g_p^{a_1 a_2} g_p^{b_1 b_2} + \dots \right). \quad (4.22)$$

which for this case gives

$$\begin{aligned} S_{F^2} &= -\kappa_7 \Omega_3 \int dx^\mu dv \sqrt{\frac{u_\Lambda^2 + v^2}{R^2}} \frac{R^3}{4g_s} \left(\sqrt{\frac{u_\Lambda^2 + v^2}{R^2}}^{-2} F_{\mu\nu} F^{\mu\nu} + 2F_{\mu\nu} F^{\mu}_v \right) \\ &= -\frac{\kappa_7 \Omega_3 R^3}{g_s} \int dx^\mu dv \frac{1}{4} \left(F_{\mu\nu} F^{\mu\nu} + 2\sqrt{\frac{u_\Lambda^2 + v^2}{R^2}} F_{\mu\nu} F^{\mu}_v \right). \end{aligned} \quad (4.23)$$

The equations of motion read

$$\partial_\mu F^{\mu\nu} + \partial_\nu F^{\nu\mu} = 0 \leftrightarrow \partial^\mu F_{\mu\nu} + \partial_\nu \left(\frac{u_\Lambda^2 + v^2}{R^2} F_{\nu\mu} \right) = 0 \quad (4.24)$$

$$\partial_\mu F^{\mu\nu} = 0 \leftrightarrow \partial^\mu F_{\mu\nu} = 0. \quad (4.25)$$

As before we expand

$$A_\mu = \sum_n B_\mu^{(n)}(x)\psi_n(v), \quad A_v = \sum_n \pi_n(x)\phi_n(v) \quad (4.26)$$

and gauge fix $\partial^\mu B_\mu = 0$ to find

$$\sum_n \partial^\mu \partial_\mu B_\nu^{(n)} \psi_n + \partial_v \left(\frac{u_\Lambda^2 + v^2}{R^2} \partial_v \psi_n \right) B_\nu^{(n)} = 0 \quad (4.27)$$

$$\partial_v \left(\frac{u_\Lambda^2 + v^2}{R^2} \partial_v \pi_0 \phi_0 \right) = 0 \rightarrow \phi_0 \propto \frac{1}{1 + \frac{v^2}{u_\Lambda^2}}. \quad (4.28)$$

In this case, the eigenvalue problem is

$$\partial_V \left((1 + V^2) \partial_V \psi_n(V) \right) = -M_{A,n}^2 \psi_n(V). \quad (4.29)$$

where again $V = \frac{v}{u_\Lambda}$.

We change to Schrödinger form via

$$V = \sinh(K) \quad (4.30)$$

$$\psi_n(K) = \frac{1}{\sqrt{\cosh(K)}} \Psi_n(K) \quad (4.31)$$

and find

$$\left(\partial_K^2 - \frac{1}{4} \left(1 + \frac{1}{\cosh(K)^2} \right) \right) \Psi_n(K) = -M_{A,n}^2 \Psi_n(K) \quad (4.32)$$

which obviously has no normalizable states. Note that the eigenvalue problem is actually the same as the M_w problem above (with a shift in the potential). Hence, the only 4D meson from this sector is again the massless pion π_0 .

4.3 Baryons

We now turn to the question of determining the size of the baryon, and for concreteness, we will model this by an instanton in the $U(N)$ gauge field living on the brane. The size of the baryon will be stabilized by the presence of the CS term as in the SS model [7, 32]. We will only use the above quadratic action plus the CS term arising from the term

$$S_{CS} = \mp \kappa_7 \int \text{Tr} (\exp(F)) \wedge C_2 \quad (4.33)$$

where C_2 is the potential leading to F_3 of the background, and further $F = dA - i[A, A]$ is the $U(N_f)$ field strength. The appropriate term is the F^3 term. We rescale F by the canonical factor of $2\pi\alpha'$, and integrate by parts to find that

$$S_{CS} = \mp \kappa_7 \frac{1}{3!} (2\pi\alpha')^3 \int \omega_5(A) \wedge F_3 = \mp \frac{N_c}{24} \int \omega_5(A) \quad (4.34)$$

where

$$\omega_5(A) = \text{Tr} \left(A F^2 - \frac{i}{2} A^3 F - \frac{1}{10} A^5 \right) \quad (4.35)$$

and the integration is now five dimensional. This is exactly the term found in [32]. We now turn to the quadratic action

$$S_{F^2} = -\frac{\kappa_7 \Omega_3 R^3}{g_s} \int dx^\mu dv \frac{1}{2} \text{Tr} \left(F_{\mu\nu} F^{\mu\nu} + 2\sqrt{\frac{u_\Lambda^2 + v^2}{R^2}} F_{\mu\nu} F^{\mu\nu} \right) \quad (4.36)$$

and perform the coordinate transformation $x^\mu = R\hat{x}^\mu$, $v = u_\Lambda V$, and further scale F by $2\pi\alpha'$ to find

$$\begin{aligned} S_{F^2} &= -\frac{\kappa_7 \Omega_3 R^3 u_\Lambda (2\pi\alpha')^2}{g_s} \int d\hat{x}^\mu dV \frac{1}{2} \text{Tr} (F_{\mu\nu} F^{\mu\nu} + 2(1+V^2) F_{\mu V} F^{\mu V}) \\ &= -\frac{u_\Lambda}{2(2\pi)^3 \sqrt{\alpha'}} \frac{(g_s N_c)^{\frac{3}{2}}}{g_s} \int d\hat{x}^\mu dV \frac{1}{2} \text{Tr} (F_{\mu\nu} F^{\mu\nu} + 2(1+V^2) F_{\mu V} F^{\mu V}) \end{aligned} \quad (4.37)$$

where μ, ν indices are still raised and lowered by $\eta_{\mu\nu}$. We will drop the $\hat{}$ in the following, knowing that V is measured in u_Λ units and x^μ is measured in R units. Note that in the limit that $V \rightarrow 0$ that the above action goes to that of the free 5D Yang-Mills (YM) theory, as it does in [32]. We therefore write down the combined action

$$S = S_{F^2} + S_{CS}. \quad (4.38)$$

Next, we wish to consider the mass of the baryon to leading order in a “small size” expansion. We will do this for the SU(2) BPST instanton by checking the energy as a function of the instanton size. The BPST instanton configuration is

$$F_{ij} = \frac{2\rho^2}{(\xi^2 + \rho^2)^2} \epsilon_{ija} \tau^a, \quad F_{iV} = \frac{2\rho^2}{(\xi^2 + \rho^2)^2} \tau_i, \quad \xi = \sqrt{(\vec{x} - \vec{x}_0)^2 + (V - V_0)^2}. \quad (4.39)$$

The constants (\vec{x}_0, V_0) parameterize the location and ρ parameterizes the size. Above, τ^i are the Pauli matrices that satisfy $\text{Tr}(\tau^a \tau^b) = 2\delta^{ab}$. We plug this into the Lagrangian density, and integrate to give the energy of this configuration (measured in units of R , as we must “unscale” time to get something with units)

$$\begin{aligned} E(\rho, V_0)R &= \frac{u_\Lambda}{2(2\pi)^3 \sqrt{\alpha'}} \frac{(g_s N_c)^{\frac{3}{2}}}{g_s} \int d^3\hat{x} dV \frac{1}{2} \text{Tr} (F_{ij} F^{ij} + 2(1+V^2) F_{iV} F^{iV}) \\ &= \frac{u_\Lambda}{2(2\pi)^3 \sqrt{\alpha'}} \frac{(g_s N_c)^{\frac{3}{2}}}{g_s} \int dV \frac{3\rho^4 \pi^2 (2+V^2)}{((V-V_0)^2 + \rho^2)^{\frac{5}{2}}} \\ &= \frac{u_\Lambda}{2(2\pi)^3 \sqrt{\alpha'}} \frac{(g_s N_c)^{\frac{3}{2}}}{g_s} (4\pi^2 V_0^2 + 2\pi^2 \rho^2 + 8\pi^2) \end{aligned} \quad (4.40)$$

which is only minimized at $V_0 = 0$ and $\rho = 0$.

Note that the above energy is the mass of the baryon in this model, which, plugging in $R = \sqrt{N_c \alpha' g_s}$ above gives

$$E(0, 0) = M_b = \frac{N_c u_\Lambda}{2\pi\alpha'}. \quad (4.41)$$

This is exactly reproduced by the energy of a D3 wrapping the S^3 (sitting at $u = u_\Lambda$) in the geometry,

$$\begin{aligned} \kappa_3 \int e^{-\phi} \det(g_p) &= (2\pi)^{-3} (\alpha')^2 \int dx^0 d\Omega_3 \frac{R}{u_\Lambda g_s} \sqrt{R^2 u_\Lambda^4} \\ &= (2\pi)^{-3} (\alpha')^{-2} 4\pi^2 \frac{R^2}{g_s} u_\Lambda \int dx^0 = \frac{N_c u_\Lambda}{2\pi \alpha'} \int dx^0. \end{aligned} \quad (4.42)$$

Before we address the effect of the CS term on the size of the baryon, we first wish to identify a perturbative parameter that will make the F^2 term parametrically larger than the CS term. To do so, we note that the coefficient of the F^2 term as

$$S_{F^2} = \frac{(u_\Lambda^2 R^2)^{\frac{1}{2}}}{\alpha'} \frac{24}{2(2\pi)^3} \frac{N_c}{24} \int d\hat{x}^\mu dV \frac{1}{2} \text{Tr} (F_{\mu\nu} F^{\mu\nu} + 2(1 + V^2) F_{\mu V} F^{\mu V})$$

and so the relative coefficient is $\frac{(u_\Lambda^2 R^2)^{\frac{1}{2}}}{\alpha'} \frac{24}{2(2\pi)^3} \equiv \hat{\lambda}$. We use this as the large parameter that we will be expanding in. We expect corrections in the size of the instanton to be of order $\lambda^{-\frac{1}{2}}$. With this in mind we scale the spatial dimensions by

$$\hat{x}^i = \hat{\lambda}^{-\frac{1}{2}} \tilde{x}^i \quad i \in \{1 \dots 3\}, \quad V = \hat{\lambda}^{-\frac{1}{2}} \tilde{V}. \quad (4.43)$$

The discussion now exactly mirrors that of the discussion in [32], with the replacement in their formulas of $a = 1/24$. Further, the parameter Z in their equations must match the appearance of V_0 in our calculation above. Therefore, we simply use their result with the appropriate changes

$$M_b = \frac{N_c u_\Lambda}{2\pi \alpha'} \left(1 + \hat{\lambda}^{-1} \left(\frac{\tilde{V}_0^2}{2} + \frac{\tilde{\rho}^2}{4} + \frac{1}{320\pi^4 a^2} \frac{1}{\tilde{\rho}^2} \right) + \mathcal{O}(\hat{\lambda}^{-2}) \right) \quad (4.44)$$

where above we have emphasized the scaling with $\hat{\lambda}$ by including the tilde, i.e. $\tilde{V}_0 = \hat{\lambda}^{\frac{1}{2}} \times V_0$, and as we have mentioned before, $a = \frac{1}{24}$. This gives that

$$\tilde{\rho}^2 = \frac{6}{\sqrt{5}\pi} \rightarrow \rho^2 = \frac{6}{\sqrt{5}\pi} \frac{1}{\hat{\lambda}} \quad (4.45)$$

To restore units, we note that one must include a factor of R in the above to get the order of the radius in the x^i directions. This gives a final result of

$$\rho_x^2 = \frac{6}{\sqrt{5}\pi} \frac{1}{\hat{\lambda}} R^2 = \frac{4}{\sqrt{5}} \pi^2 \frac{R}{u_\Lambda} \alpha'. \quad (4.46)$$

Physical length in this background near the point $u = u_\Lambda$ is measured in $dx^2/(R/u_\Lambda)$ units. Therefore, the physical size of the above distribution is $\frac{2\pi}{5^{1/4}} \sim 4.2$ in string units. This is not very big, and so string corrections may be needed.

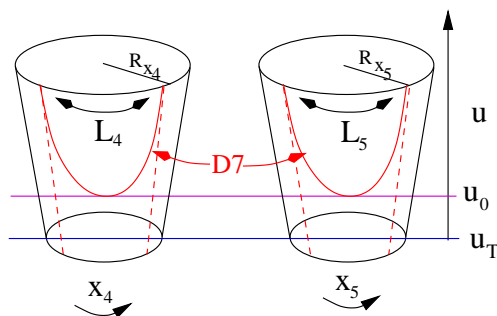


Figure 7. The configuration of D7 branes in the near extremal D5 brane background with the thermal factor on the time component of the metric. The dashed lines show a possible configuration with the branes falling into the horizon.

5 Deconfined phase

One may also wish to study the physics of the phase where the blackening factor f appears on the timelike component of the metric. For such a background, we have

$$ds^2 = \frac{u}{R} (-f(u; u_T) dt^2 + \delta_{ij} dx^i dx^j + dx_4^2 + dx_5^2) + \frac{R}{u} \frac{du^2}{f(u; u_T)} + R u d\Omega_3^2 \quad (5.1)$$

and

$$\exp \phi = g_s \frac{u}{R}, \quad F_3 = \frac{2R^2}{g_s} \Omega_3. \quad (5.2)$$

In this case u_T implies a horizon, however, classically the temperature does not depend on this parameter at all (as the periodicity of x_5 in the last section). Here

$$\delta t = 2\pi R = \frac{1}{T}, \quad (5.3)$$

and further, we can take u_T to be a measure of the energy density via

$$E(u_T) = u_T^2 \frac{V_5}{(2\pi)^5 (\alpha')^4 g_s^2}, \quad S = 2\pi R E(u_T). \quad (5.4)$$

Above we have used the energy as measured for a near extremal D5 in flat $\mathbb{R}^{1,9}$, and S is obtained via the Bekenstein-Hawking formula.

As in the last section, one can take the embedding of a D7 which is transverse to some combination of u, x_4, x_5 . Possible configurations are shown graphically in figure 7.

Again, choosing u to be the world volume coordinate of the brane ρ , we find the reduced action

$$\frac{T_8}{g_s} V_4 V_3 \int d\rho \rho^3 \sqrt{f(\rho; u_T) ((\partial x_4)^2 + (\partial x_5)^2) + \frac{R^2}{\rho^2}}. \quad (5.5)$$

As before, we find the conserved quantities

$$\frac{\rho^3 f(\rho; u_T) \partial x_4}{\sqrt{f(\rho; u_T) ((\partial x_4)^2 + (\partial x_5)^2) + \frac{R^2}{\rho^2}}} = P_4 u_T^3 \quad (5.6)$$

$$\frac{\rho^3 f(\rho; u_T) \partial x_5}{\sqrt{f(\rho; u_T) ((\partial x_4)^2 + (\partial x_5)^2) + \frac{R^2}{\rho^2}}} = P_5 u_T^3 \quad (5.7)$$

which allows us to solve for $\partial x_4, \partial x_5$ as

$$\hat{\partial}x_4 = R \frac{P_4}{\sqrt{\hat{\rho}^2 f(\hat{\rho}; 1) (\hat{\rho}^6 f(\hat{\rho}; 1) - (P_4^2 + P_5^2))}} \quad (5.8)$$

$$\hat{\partial}x_5 = R \frac{P_5}{\sqrt{\hat{\rho}^2 f(\hat{\rho}; 1) (\hat{\rho}^6 f(\hat{\rho}; 1) - (P_4^2 + P_5^2))}}. \quad (5.9)$$

where in this section we define

$$\hat{\rho} = \frac{\rho}{u_T}, \quad \hat{\partial} = \frac{\partial}{\partial \hat{\rho}} \quad (5.10)$$

This allows us to immediately identify

$$P_4^2 + P_5^2 \equiv P^2 \equiv \hat{\rho}_0^6 \left(1 - \frac{1}{\hat{\rho}_0^2}\right) \quad (5.11)$$

where $\hat{\rho}_0$ is the minimal value to which the brane falls ($\hat{\rho}_0 = \rho_0/u_T = u_0/u_T$). We note that the action is a function only of $\hat{\rho}_0$. The above configurations always give a connected brane antibrane for $P^2 > 1$.

Further, we should note that because the functions $\frac{L_i(\hat{\rho}_0)}{R}$ only depend on $\hat{\rho}_0$, that for fixed boundary condition at infinity, varying u_Λ does not affect $\hat{\rho}_0$. This is because to maintain the boundary conditions at infinity, one must vary u_0 in just such a way as to keep $u_0/u_T = \hat{\rho}_0$ fixed.

One may now ask whether the connected configuration (considered above) is preferred or whether the configuration where the brane anti-brane pair simply fall into the horizon is preferred. To measure this, we subtract the two (infinite) actions, considering the boundary conditions as being placed at some finite (but large) value of u , and then relaxing this position to infinity. This defines our regularization procedure.

The resulting difference we wish to consider is therefore

$$\begin{aligned} \frac{\Delta S}{2V_3 V_4 T_7 R u_T^3} &= \int_{\hat{\rho}_0}^{\infty} d\hat{\rho} \hat{\rho}^5 \sqrt{\frac{f(\hat{\rho}; 1)}{\hat{\rho}^6 f(\hat{\rho}; 1) - \hat{\rho}_0^6 f(\hat{\rho}_0; 1)}} - \int_1^{\infty} d\hat{\rho} \hat{\rho}^2 \\ &= \int_{\hat{\rho}_0}^{\infty} d\hat{\rho} \left(\hat{\rho}^5 \sqrt{\frac{f(\hat{\rho}; 1)}{\hat{\rho}^6 f(\hat{\rho}; 1) - \hat{\rho}_0^6 f(\hat{\rho}_0; 1)}} - \hat{\rho}^2 \right) - \frac{1}{3}(\hat{\rho}_0^3 - 1). \end{aligned} \quad (5.12)$$

We cannot evaluate this exactly, however, we may plot it numerically. The plot shows that for $\frac{u_0}{u_T} < \hat{\rho}_0^c \approx 2.4456$ that the separated D7 $\overline{\text{D7}}$ is preferred, and that for $\frac{u_0}{u_T} > \hat{\rho}_0^c \approx 2.4456$ that the connected ‘‘U-shaped’’ configuration is preferred. Because the temperature is not a function of u_T , we may not associate this with a phase transition, even in the space of energy density, of which u_T is a measure. To stress this point, we may easily plug this into the equations for L_4 and L_5 and find

$$L(\hat{\rho}_0^c) \equiv \sqrt{L_4(\hat{\rho}_0^c)^2 + L_5(\hat{\rho}_0^c)^2} = 1.068R. \quad (5.13)$$

We note that in the above R does not vary as we vary u_T , and neither does L (as this is a boundary condition we are imposing). We find therefore that the chiral symmetry

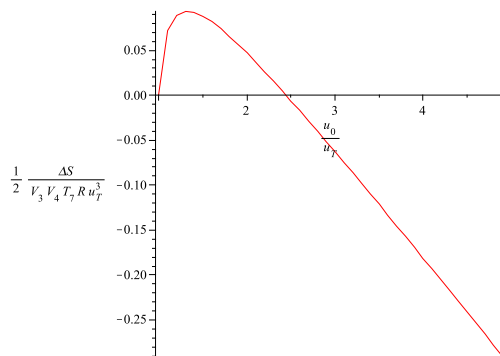


Figure 8. The difference in actions between the “U-shaped” and “|-shaped” configurations plotted as a function of $\hat{\rho}_0 = \frac{u_0}{u_T}$.

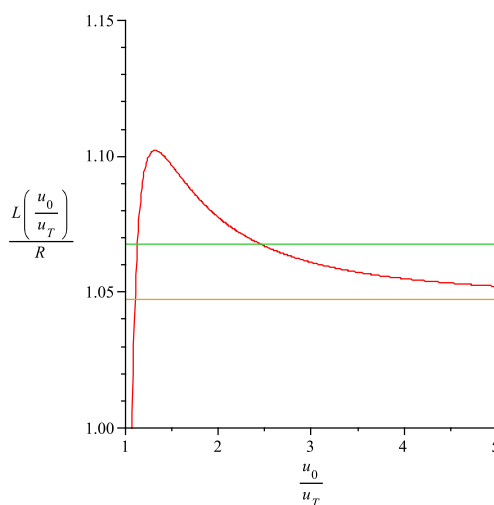


Figure 9. $\frac{L(\hat{\rho}_0 = \frac{u_0}{u_T})}{R}$ along with the critical value $\frac{L(\hat{\rho}_0^c \approx 2.4456)}{R} \approx 1.068$, and the asymptotic value of $\frac{L(\hat{\rho}_0 = \infty)}{R} = \frac{\pi}{3} \approx 1.047$, plotted as red green and yellow respectively. Although we have not plotted it, the remainder of the graph for $\frac{L(\hat{\rho}_0)}{R}$ goes to zero as $\hat{\rho}_0 \rightarrow 1$.

breaking/restoration is purely a function of the boundary conditions imposed, and find that for $\frac{\pi}{3}R < L \lesssim 1.068R$ that chiral symmetry is present in the deconfining phase, and that for $L \gtrsim 1.068R$ chiral symmetry is broken in the deconfining phase. However, we note that if $L < \frac{\pi}{3}R$ that chiral symmetry is again broken (unless there is some problem with an open string tachyon, to which our analysis is insensitive). We plot the curve of $\frac{L(\hat{\rho}_0)}{R}$ along with the critical value $\frac{L(\hat{\rho}_0^c)}{R} \approx 1.068$, and the asymptotic value of $\frac{L(\hat{\rho}_0 = \infty)}{R} = \frac{\pi}{3} \approx 1.047$ in figure 9 to make this more clear. One can therefore see that outside the window $\frac{\pi}{3}R < L \lesssim 1.068R$, chiral symmetry is broken. When L is above this window, the brane dips far enough towards the horizon that the separated brane configuration is preferred. However, this also occurs below $\frac{\pi}{3}R$: if the asymptotic separation is below this value, there does exist a value of $\hat{\rho}_0$ which allows for a connected configuration, however in this case $\hat{\rho}_0$ is always less

than $\hat{\rho}_0^c$, and so the separated configuration is preferred. It may be, however, that there are no solutions with $L < \frac{\pi}{3}$, and that the disconnected solution is only a local minimum. One could argue this by starting with L very large and bringing the branes together. It is possible to tunnel from the disconnected to connected solution once $L \gtrsim 1.068R$. Then as one brings the ends closer together, the value of u_0 runs off to infinity. In fact, from the plot in figure 8, it suggests that the effective potential is running off to $-\infty$ for smaller and smaller values of L . This suggests that the solutions for $L < \frac{\pi}{3}$ are only classically stable, similar to starting with an “inverted wine bottle” $\phi^2 - \phi^4$, and taking $\phi = 0$ as a solution (when, in fact, it will tunnel out because the potential is unbounded from below). We therefore take that there are no solutions for $L \leq \frac{\pi}{3}R$; for $\frac{\pi}{3}R < L \lesssim 1.068R$, chiral symmetry is broken; and that for $L \gtrsim 1.068R$ that chiral symmetry is broken. This similar to the results of [9] where chiral symmetry was broken for $L < 0.97R$ and restored for $L > 0.97R$.

6 Conclusions, and outlook

The above model offers a new dual description of a model in the same universality class as large N_c QCD with flavors, different from that of the SS model [1, 7, 8]. There are certain notable similarities and differences. First, the temperature dependence of the theory is quite striking: a thermal “black brane” background is only available at a specific temperature $T = \frac{1}{2\pi R}$. Further, in the deconfined phase, the boundary conditions $\frac{L_i}{R}$ are functions only of the ratio $\frac{u_0}{u_T}$. This has the interesting quality of making solutions with the same boundary conditions at infinity easy to find: if one scales u_T by a factor C , then one must also scale u_0 by C . This has the effect that varying u_Λ with constant boundary conditions yields no phase transitions: either chiral symmetry is always broken or restored, simply given the boundary conditions. This allows for the possibility of making such a phase transition simultaneous. Finally, we should also note the appearance of a finite height effective potential in the radial direction, giving a finite number of 4D mesons, unlike the case of SS.

There are also some striking similarities. The mechanism for chiral symmetry breaking in the confined phase is identical to that of the SS model, and easy to visualize. Further, considering the baryons as instantons in the $U(N_f)$ world volume gauge field on the D7, an almost identical mechanism for the baryon size being stabilized arises, and in both cases the size is of the string scale.

The biggest drawback of our model is the far to simple spectrum of mesons, resulting from the finite height and flattening of all effective potentials. One may wish to see how one could modify this setup to allow for a larger spectrum of mesons, possibly for different values of boundary conditions. More specifically, in the confining phase, it would be interesting to see what effect turning on P_4 would have. Recall that in the anti-podal embedding, the minimum of the effective potential is reached when the brane reaches all the way down to u_Λ . Further, recall that introducing a non zero P_4 does not change this: the brane still reaches the minimal value $u_0 = u_\Lambda$. So, in such a situation, more effective world volume of the brane exists near where the bottom of the effective potential exists, possibly widening the bottom of the effective potential, and leading to more bound states. Such

an analysis, however, could be quite involved and need to rely on numerical methods. A further drawback is the possible quantum mechanical instability of the system. It would be interesting to find solutions to this as well, for example whether the backreaction of the flavor branes could help cure this problem.

Given the vast number of analysis works of the SS background, there remains many possibilities for future work. For example, one may be curious to study the meson spectrum in the deconfining phase similar to [10], particularly to see if one finds similar patterns to the meson melting found via quasi-normal mode analysis [33], as well as modeling the condensation of various modes as in [14]. Also, including bare quark mass will have to follow similar lines as those in the SS model [15, 34], and studies with such deformations. We have also not addressed any possible transition between the deconfined and confined phase. In fact, one should imagine tuning the temperature (in the confined phase) all the way up to $T = \frac{1}{2\pi R}$. Since this is the only temperature that admits two different solutions (with the blackening factor) this is the only possible temperature at which a phase transition happens. Note that quantum mechanically the region $T > \frac{1}{2\pi R}$ does not exist due the Hagedorn instability (neglecting the backreaction of the flavor branes). Such a phase transition at $T = \frac{1}{2\pi R}$ would be driven simply by the presence of the flavors (as the two Euclidean actions would be identical for the gravity sector). We would then have to subtract the two DBI actions with identical boundary conditions at infinity, but with the blackening factor on different components of the metric. Inverting the relation between the boundary conditions L_i and the P_i is, however, not straightforward. We hope to return to these questions in the future.

Acknowledgments

We wish to thank Ofer Aharony for participating in the early stages of this work, useful discussions and for his remarks on the manuscript. BB also wishes to thank Gaetano Bertoldi for useful discussions. The work of BB is supported by NSERC of Canada. The work of J.S was supported in part by a center of excellence supported by the Israel Science Foundation (grant number 1468/06), by a grant (DIP H52) of the German Israel Project Cooperation, by a BSF grant and by the European Network MRTN-CT-2004-512194.

References

- [1] E. Witten, *Anti-de Sitter space, thermal phase transition and confinement in gauge theories*, *Adv. Theor. Math. Phys.* **2** (1998) 505 [[hep-th/9803131](#)] [[SPIRES](#)].
- [2] J.M. Maldacena, *The large- N limit of superconformal field theories and supergravity*, *Adv. Theor. Math. Phys.* **2** (1998) 231 [*Int. J. Theor. Phys.* **38** (1999) 1113] [[hep-th/9711200](#)] [[SPIRES](#)].
- [3] O. Aharony, S.S. Gubser, J.M. Maldacena, H. Ooguri and Y. Oz, *Large- N field theories, string theory and gravity*, *Phys. Rept.* **323** (2000) 183 [[hep-th/9905111](#)] [[SPIRES](#)].
- [4] A. Karch and E. Katz, *Adding flavor to AdS/CFT*, *JHEP* **06** (2002) 043 [[hep-th/0205236](#)] [[SPIRES](#)].

- [5] T. Sakai and J. Sonnenschein, *Probing flavored mesons of confining gauge theories by supergravity*, *JHEP* **09** (2003) 047 [[hep-th/0305049](#)] [[SPIRES](#)].
- [6] J. Erdmenger, N. Evans, I. Kirsch and E. Threlfall, *Mesons in Gauge/Gravity Duals - A Review*, *Eur. Phys. J. A* **35** (2008) 81 [[arXiv:0711.4467](#)] [[SPIRES](#)].
- [7] T. Sakai and S. Sugimoto, *Low energy hadron physics in holographic QCD*, *Prog. Theor. Phys.* **113** (2005) 843 [[hep-th/0412141](#)] [[SPIRES](#)].
- [8] T. Sakai and S. Sugimoto, *More on a holographic dual of QCD*, *Prog. Theor. Phys.* **114** (2005) 1083 [[hep-th/0507073](#)] [[SPIRES](#)].
- [9] O. Aharony, J. Sonnenschein and S. Yankielowicz, *A holographic model of deconfinement and chiral symmetry restoration*, *Annals Phys.* **322** (2007) 1420 [[hep-th/0604161](#)] [[SPIRES](#)].
- [10] K. Peeters, J. Sonnenschein and M. Zamaklar, *Holographic melting and related properties of mesons in a quark gluon plasma*, *Phys. Rev. D* **74** (2006) 106008 [[hep-th/0606195](#)] [[SPIRES](#)].
- [11] O. Bergman, S. Seki and J. Sonnenschein, *Quark mass and condensate in HQCD*, *JHEP* **12** (2007) 037 [[arXiv:0708.2839](#)] [[SPIRES](#)].
- [12] A. Dhar and P. Nag, *Sakai-Sugimoto model, Tachyon Condensation and Chiral symmetry Breaking*, *JHEP* **01** (2008) 055 [[arXiv:0708.3233](#)] [[SPIRES](#)].
- [13] A. Dhar and P. Nag, *Tachyon condensation and quark mass in modified Sakai-Sugimoto model*, *Phys. Rev. D* **78** (2008) 066021 [[arXiv:0804.4807](#)] [[SPIRES](#)].
- [14] O. Aharony, K. Peeters, J. Sonnenschein and M. Zamaklar, *Rho meson condensation at finite isospin chemical potential in a holographic model for QCD*, *JHEP* **02** (2008) 071 [[arXiv:0709.3948](#)] [[SPIRES](#)].
- [15] O. Aharony and D. Kutasov, *Holographic Duals of Long Open Strings*, *Phys. Rev. D* **78** (2008) 026005 [[arXiv:0803.3547](#)] [[SPIRES](#)].
- [16] R. McNees, R.C. Myers and A. Sinha, *On quark masses in holographic QCD*, *JHEP* **11** (2008) 056 [[arXiv:0807.5127](#)] [[SPIRES](#)].
- [17] P.C. Argyres, M. Edalati, R.G. Leigh and J.F. Vazquez-Poritz, *Open Wilson Lines and Chiral Condensates in Thermal Holographic QCD*, *Phys. Rev. D* **79** (2009) 045022 [[arXiv:0811.4617](#)] [[SPIRES](#)].
- [18] M. Edalati, R.G. Leigh and N.N. Hoang, *Transversely-intersecting D-branes at finite temperature and chiral phase transition*, *JHEP* **05** (2009) 035 [[arXiv:0803.1277](#)] [[SPIRES](#)].
- [19] E. Antonyan, J.A. Harvey and D. Kutasov, *Chiral symmetry breaking from intersecting D-branes*, *Nucl. Phys. B* **784** (2007) 1 [[hep-th/0608177](#)] [[SPIRES](#)].
- [20] O. Aharony, A. Giveon and D. Kutasov, *LSZ in LST*, *Nucl. Phys. B* **691** (2004) 3 [[hep-th/0404016](#)] [[SPIRES](#)].
- [21] O. Aharony, M. Berkooz, D. Kutasov and N. Seiberg, *Linear dilatons, NS5-branes and holography*, *JHEP* **10** (1998) 004 [[hep-th/9808149](#)] [[SPIRES](#)].
- [22] D. Kutasov, *Introduction To Little String Theory*, Prepared for ICTP Spring School on Superstrings and Related Matters, Trieste, Italy, 2–10 Apr 2001 [[SPIRES](#)].
- [23] D. Marolf and A. Virmani, *Holographic Renormalization of Gravity in Little String Theory Duals*, *JHEP* **06** (2007) 042 [[hep-th/0703251](#)] [[SPIRES](#)].

- [24] A. Parnachev and A. Starinets, *The silence of the little strings*, *JHEP* **10** (2005) 027 [[hep-th/0506144](#)] [[SPIRES](#)].
- [25] S. Elitzur, A. Giveon, D. Kutasov, E. Rabinovici and G. Sarkissian, *D-branes in the background of NS fivebranes*, *JHEP* **08** (2000) 046 [[hep-th/0005052](#)] [[SPIRES](#)].
- [26] S.L. Lukyanov, E.S. Vitchev and A.B. Zamolodchikov, *Integrable model of boundary interaction: The paperclip*, *Nucl. Phys. B* **683** (2004) 423 [[hep-th/0312168](#)] [[SPIRES](#)].
- [27] D. Kutasov, *D-brane dynamics near NS5-branes*, [hep-th/0405058](#) [[SPIRES](#)].
- [28] M. Kruczenski, L.A.P. Zayas, J. Sonnenschein and D. Vaman, *Regge trajectories for mesons in the holographic dual of large- N_c QCD*, *JHEP* **06** (2005) 046 [[hep-th/0410035](#)] [[SPIRES](#)].
- [29] E. Antonyan, J.A. Harvey, S. Jensen and D. Kutasov, *NJLS and QCD from string theory*, [hep-th/0604017](#) [[SPIRES](#)].
- [30] H. Stephani, *Differential equations: Their solution using symmetries*, Cambridge University Press, Cambridge U.K. (1989).
- [31] S. Kuperstein and J. Sonnenschein, *A New Holographic Model of Chiral Symmetry Breaking*, *JHEP* **09** (2008) 012 [[arXiv:0807.2897](#)] [[SPIRES](#)].
- [32] H. Hata, T. Sakai, S. Sugimoto and S. Yamato, *Baryons from instantons in holographic QCD*, [hep-th/0701280](#) [[SPIRES](#)].
- [33] C. Hoyos-Badajoz, K. Landsteiner and S. Montero, *Holographic Meson Melting*, *JHEP* **04** (2007) 031 [[hep-th/0612169](#)] [[SPIRES](#)].
- [34] K. Hashimoto, T. Hirayama, F.-L. Lin and H.-U. Yee, *Quark Mass Deformation of Holographic Massless QCD*, *JHEP* **07** (2008) 089 [[arXiv:0803.4192](#)] [[SPIRES](#)].